



The Scarlet Solar Array: Technology Validation and Flight Results

David M. Murphy
dmurphy@aec-able.com

AEC-Able Engineering Co., Inc
www.aec-able.com

Tel: 805.685.2262



AECABLE



JPL
Schafer

Deep Space 1 Technology Validation Report

Table of Contents

Section	Description	Page
1. EXTENDED ABSTRACT		1
2. INTRODUCTION		3
3. TECHNOLOGY DESCRIPTION		3
3.1 Overview.....		3
3.2 Key Validation Objectives at Launch		3
3.3 Expected Performance Envelope		4
3.4 Detailed Design Description		5
3.4.1 Overview.....		5
3.4.2 Mechanical Description		5
3.4.3 Electrical Description.....		5
3.4.4 Optical Description.....		6
3.4.5 Thermal Design.....		7
3.5 Technology Interdependencies.....		8
3.6 Test Program.....		8
3.6.1 Ground Test Validation		8
3.6.2 Flight Test Validation		10
3.7 Analysis of Flight Test Results.....		10
3.7.1 Deployment.....		10
3.7.2 Pointing.....		12
3.7.3 Temperature		13
3.7.4 Power		15
4. TECHNOLOGY VALIDATION SUMMARY		18
5. APPLICATION FOR FUTURE MISSIONS		19
6. ACKNOWLEDGMENTS.....		19
7. REFERENCES		19

Figures

Figure 1. One wing of <i>Scarlet</i> for DS1 showing module level details: Lens, Frame, and Photovoltaic Receiver ...	1
Figure 2. DS1 <i>Scarlet</i> (Wing 1 of 2) on Deploy Rail	3
Figure 3. DS1 Mission Timeline vs Sun Distance	4
Figure 4. <i>Scarlet</i> Module: Lens and Receiver.....	5
Figure 5. DS1 <i>Scarlet</i> Wing	5
Figure 6. Temperature Profile Across Cell.....	7
Figure 7. Temperature Profile Across Panel (From cell center to centerline between module rows).....	7
Figure 9. <i>Scarlet</i> String I-V Curves	9
Figure 10. Ascent to Deployment Temp. Transient.....	11
Figure 11. Deployment Duration vs. Temperature	12
Figure 12. Light Collection versus Alpha Angle	12
Figure 13. Pointing Validation Summary	12
Figure 14. RTDs: 4 on a Module (in 2 Locations).....	13
Figure 15. Thermal Modeling Results for 1.0174 AU.....	13
Figure 16. Steady State Temperature vs. Power Draw.....	14
Figure 17. Short Circuit Current Degradation	15
Figure 18. Historical Sunspot Activity	16
Figure 19. Tap Module - Wing 1, Panel 1	16
Figure 20. SPeak Sequence Flight Data	16
Figure 21. SPeak Sequence, Incrementing Voltage Near Peak Power	16
Figure 22. SPeak Data, Array Output at 1.1185 AU.....	17

Table of Contents

Section	Description	Page
Figure 23.	Mini-SPeak 1, Mission Day 160	17
Figure 24.	Mini-SPeak 1, Peak IV Data.....	17
Figure 25.	Original Forecasts and Flight Data	18

Tables

Table 1.	Optical Losses in Lens Assy.....	7
Table 2.	Random Vibration Test Levels.....	9
Table 3.	Protoqual Deploy Timing Ranges.....	11
Table 4.	Flight Release and Deploy Durations.....	11

Appendices

Appendix A	Telemetry Channels Related to Array Technology Validation.....	A-1
Appendix B	In-Flight Array Validation Activities and Data Summary	B-1

The Scarlet Solar Array: Technology Validation and Flight Results

1. EXTENDED ABSTRACT

The Solar Concentrator Arrays with Refractive Linear Element Technology (SCARLET) system used on the Deep Space 1 (DS1) spacecraft has been validated through successful performance in flight. *Scarlet*TM is the first successful concentrator array ever used as primary power for a spacecraft.

Flight results to date show that performance projections were within 1% of measured results, making *Scarlet* one of the highest performance solar arrays ever used in space. The *Scarlet* array uses linear, arched Fresnel lens concentrators to focus sunlight onto narrow rows of multiple band gap solar cells to produce 2.5-kW of power. This paper describes the array technology, development process, array assembly and qualification, and flight operations of this novel system.

DS1, the first of the NASA New Millennium series of exploratory spacecraft, was launched in October 1998 and completed its primary mission in July 1999. The primary objective for DS1 was to test advanced technologies that can reduce the cost or risk of future missions. Although part of the advanced technology validation study, the array is also the power source for the spacecraft and its NASA Solar electric propulsion Technology Application Readiness (NSTAR) electric propulsion system. The array continues providing power to DS1 and its NSTAR ion electric propulsion system on the way to the next encounter object.

Sponsored by the Ballistic Missile Defense Organization (BMDO), the *Scarlet* concentrator solar array is the first space application of a refractive lens concentrator and the first to use both dual and triple junction solar cells. As part of the DS1 validation process, the amount of diagnostics data acquired was more extensive than would be the norm for a more conventional solar array.

These data included temperature measurements at numerous locations on the 2-wing, 4-panel per wing, solar array. For each panel, one 5-cell module in one of the circuit strings was wired to obtain complete I-V curves. The data was used to verify sun pointing accuracy and array output performance. In addition, the spacecraft power load could be varied in a number of discrete steps, from a small fraction of the array total power capability, up to maximum power. For each of the power loads, array operating voltage could be measured along with the current output from each wing.

The performance of *Scarlet* on DS1 substantially validated all aspects of the novel structural platform, Fresnel optics, multi-junction cell module performance, and electrical design. The major features of safe stowage through launch, deployment, and sun acquisition were clearly demonstrated on the first day of the mission. Stability of the array system, in particular, the ability to maintain the relatively tight pointing, has been verified over more than a year. The array performance has continued to achieve design specifications without imposing any onerous requirements on the spacecraft.

The main feature of the technology is that for a given power level, the *Scarlet* optical system reduces the required solar cell area by approximately a factor of seven. The decreased cell area can significantly reduce solar array cost while at the same time providing state-of-the-art performance. *Scarlet* allows the cost-effective implementation of advanced cell technologies, as demonstrated on DS1, especially when early production may limit availability or greatly elevate costs.

Another particular advantage of *Scarlet* is for applications with severe radiation environments where a thick cell coverglass is needed. The low cell area fraction means that thick glass won't significantly increase wing mass. This can be a mission-enabling feature for MEO orbits or for exploration at or near large planets with high trapped radiation levels. Often interplanetary missions must contend with the debilitating effect on cell performance that low light intensity and low temperature (LILT) can cause. The concentrating optics of *Scarlet* can be utilized to overcome these performance losses as well.

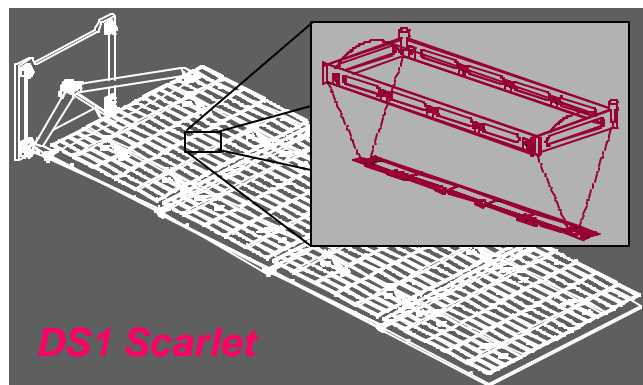


Figure 1. One wing of *Scarlet* for DS1 showing module level details: Lens, Frame, and Photovoltaic Receiver

To obtain further information on the development and commercialization of the *Scarlet* technology please contact the author, Dave Murphy, or ABLE's marketing technical director, Brian Spence, at (805) 685-2262. Learn about our past history and recent developments, such as *Scarlet* advancements, on the web at www.aec-able.com.



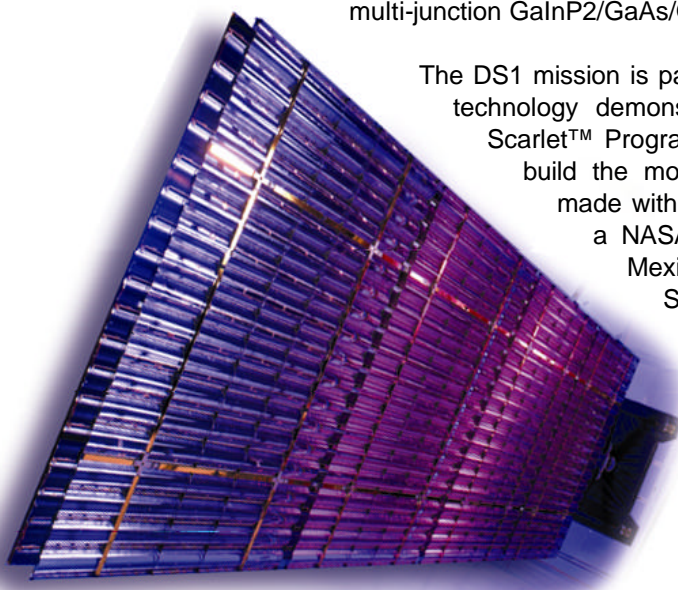
ABLE provided the Scarlet™ solar concentrator arrays for the Deep Space 1 (DS1) spacecraft. Launched October 24, 1998, the solar arrays deployed flawlessly and have operated according to pre-flight predictions ever since. DS1 is the first spacecraft primarily powered by Scarlet™ solar arrays and will rely on them to energize the electric propulsion and other systems during the full course of the mission.

LOW COST
LOW WEIGHT
RADIATION HARD



The Ballistic Missile Defense Organization sponsored Scarlet™ for use on DS1. Scarlet™ technology was developed with ENTECH, Inc, who supply the Fresnel optics, and the NASA Glenn Research Center at Lewis Field

The revolutionary Scarlet™ arrays employ a patented refractive Fresnel lens system, which concentrates sunlight onto the solar cells. Because of this, less solar cell area is required, providing tremendous weight and cost savings. Additionally, using fewer and smaller cells allowed the cost-effective implementation of high efficiency multi-junction GaInP2/GaAs/Ge photovoltaic cells aboard DS1.



The DS1 mission is part of The New Millennium Program, NASA's most aggressive technology demonstration program. According to Ray Garza, ABLE's DS1 Scarlet™ Program Manager, "This high technology mission challenged us to build the most advanced solar array in the world." Such strides were made with this new technology that ABLE was recognized in 1999 with a NASA Group Achievement Award and by the University of New Mexico's Institute for Space and Nuclear Power with their Schreiber-Spence Achievement Award.

The performance of the Scarlet™ arrays on DS1 validated all aspects of the novel structural platform, optics, and electrical design as well as the analytical models used to characterize the array. The Scarlet™ technology proven on DS1 will continue to be refined to benefit future science mission as well as commercial endeavors such as mid-level orbit satellites, and communication constellations.

DS1 SCARLET™

SPECIFICATIONS

Wing Dimensions: 206 in. x 64 in.
Panel Dimensions: 45 in. x 63 in. (4 panels per wing)
Array Power: 2500 W (1 AMO)
Wing Mass: 27.7kg (with tiedowns)

Specific Power: 45 W/kg
Stowed Stiffness: 92 Hz
Deployed Stiffness: 0.37 Hz
Deployed Strength: 0.015 g's

AEC-ABLE ENGINEERING COMPANY, INC
93 CASTILIAN DRIVE
GOLETA CA 93117

HTTP://WWW.AEC-ABLE.COM/SOLAR
E-MAIL: SOLARARRAYS@AEC-ABLE.COM
TEL: 805.685.2262 • FAX: 805.685.1369

The Scarlet Solar Array: Technology Validation and Flight Results

2. INTRODUCTION

This report summarizes the design, development, and test of the Solar Concentrator Array with Refractive Linear Element Technology (SCARLET) system and details the flight validation on the New Millennium Deep Space 1 (DS1) mission. Array deployment, system pointing, thermal performance, and power production are analyzed and discussed in comparison to ground results and mission predictions. In summary, the solar array has operated flawlessly and all aspects of the technology were successfully validated in pre-launch and mission activities.

The flight of *Scarlet* on DS1 has enabled the development and validation of a low-recurring cost technology which offers significant advantages for radiation applications, such as MEO orbits, or LILT applications. For example, missions to large outer planetary bodies can benefit from the weight efficient radiation hardness and the LILT advantages of the *Scarlet* technology. This novel flight-validated solar array is a cost-effective and mission-enabling technology.

3. TECHNOLOGY DESCRIPTION

3.1 Overview

Scarlet is a concentrator solar array for space applications which uses linear refractive Fresnel lenses to focus sunlight onto spaced rows of solar cells. For a given power level, the *Scarlet* optical system reduces the required solar cell area by approximately a factor of 7. The decreased cell area can significantly reduce solar array system cost and weight, especially in high radiation environments where thick cell coverglass is required.

The DS1 array is derived from and scaled up from the prototype *Scarlet* wing that was built for the METEOR satellite in 1995. Due to the failure of the Conestoga launch vehicle, DS1 was the first flight of *Scarlet* technology. This second-generation *Scarlet* solar array incorporated many additional advanced technologies such as multi-junction solar cells and a new mechanization and structural design.

AEC-Able Engineering Company, Inc. (ABLE), designed, assembled, and tested the 2.5 kW concentrator solar array for the DS1 mission, which launched on October 24th of 1998. The Ballistic Missile Defense Organization (BMDO) Innovative Science and

Technology Directorate has sponsored development of *Scarlet* through the first New Millennium Space flight on the Deep Space 1 spacecraft. Substantial funding support and technical aid for this application was also provided by the Jet Propulsion Laboratory (JPL).

The DS1 *Scarlet* solar array has made significant advances in the state-of-the-art of space-demonstrated solar cells, concentrators, lightweight packaging, and deployment techniques.



Figure 2. DS1 Scarlet (Wing 1 of 2) on Deploy Rail

The pioneering success of the *Scarlet* Array was recognized with the 1999 Schreiber-Spence Award for Significant Technology Advances. This year's award was presented to the NSTAR and *Scarlet* teams in recognition of the first use of solar-powered ion propulsion as primary propulsion and of the first use of a multi-band-gap, concentrator array for a robotic, deep-space mission, thereby helping to open the solar system to frequent, low-cost exploration. *Scarlet*, with its radiation hardness capability and ion propulsion employed together, also provides an excellent combination for the cost-saving concept of orbit raising from LEO.

3.2 Key Validation Objectives at Launch

Data collection objectives for technology validation were formulated for two phases of the mission. Within the first month of the mission the data desired was:

- Initial power telemetry data collection on earliest day possible using all tap circuits and temperature sensors: 8 taps and 10 Resistive Temperature Detectors (RTDs).

This data verifies initial performance prior to on-orbit calibration. RTDs were used to extrapolate cell

temperatures and to validate the array thermal design by measuring gradients in the structure around the focal line of the tap modules.

- On-orbit calibration to maximize power output of the array prior to beginning cruise phase.

This data was used to evaluate and validate the accuracy of the initial alignment of the array/spacecraft with respect to perceived attitude.

- Power telemetry data sets taken nominally every week to validate performance vs. AU, temperature, and environmental degradations.

It was important to record data often at the start of the mission to capture early degradation effects such as spacecraft or array outgassing contamination and UV darkening.

For beyond the first month the data desired was:

- Power telemetry data sets nominally every two weeks (every month as a minimum when or if mission events conflict) to validate performance vs. AU, temperature, and environmental degradations.

Regular data sets form the basis for validating and correlating power output and modeling.

Criteria for incremental success in flight validation were developed and documented in the New Millennium Program - Deep Space One Project Technology Validation Agreement between BMDO, JPL, and ABLE. Those criteria were:

- | | |
|-----|--|
| 50% | Successful zero-g deployment of both wings |
| 60% | Successful acquisition of launch and deployment activities data, Spacecraft orientation from spin-down to start of deployment event, Time history of the states of telemetry switches and RTDs |
| 75% | Successful acquisition of initial power telemetry data set, which includes: Current and voltage (IV) curve data points for each of the 8 tap circuits, Temperature readings from each of 10 RTDs, day and time, Heliocentric distance, Wing orientations: alpha for each wing and beta of spacecraft, Spacecraft orientation reference data and alpha/beta offsets |
| 80% | Successful acquisition of initial on-orbit alpha-beta calibration data |
| 90% | Produce power in excess of 2400 W at BOL |

100% Successful acquisition of periodic power production data

In summary, each of these goals was fully met, and thus, 100% success was attained, with one caveat: The "periodic" power telemetry data sets were not as numerous as planned. The spacecraft has had a series of anomalies unrelated to the solar array that caused delay and postponed *Scarlet* validation activities by several months.

As the mission has progressed, opportunities to refine the understanding of detailed modeling factors have become available. By March of 2000 the spacecraft will be back to 1.1 AU after traveling out to almost 1.35, and after nine more months will have reached 1.35 again. This mission profile, shown in Figure 3, will allow analysis to separate time and distance effects.

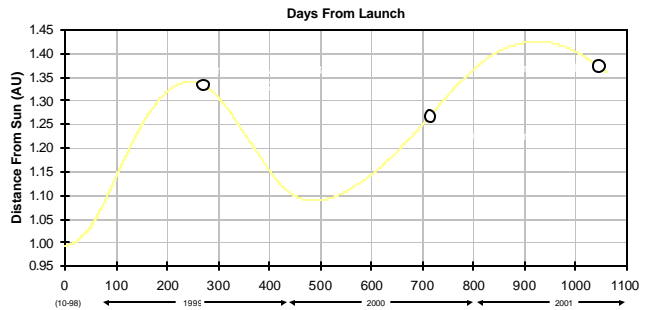


Figure 3. DS1 Mission Timeline vs Sun Distance

3.3 Expected Performance Envelope

The performance envelope of any future *Scarlet* array is well understood as many detailed point designs have been generated from the DS1 baseline. It has been configured into arrays from 500 to 25,000 W, for LEO, MEO, GEO, and interplanetary missions. The key metrics for array evaluation are specific power (W/kg) and cost. The cost advantage with concentration is self-evident, and the remaining questions for planning or selection are whether the array will meet all mission requirements and at what level of performance.

Scarlet technology has now been proven out with the flight of DS1 and the completion of subsystem qualifications tests which complete the verification of thermal cycle capability in various environments. The key measure of performance, specific power, demonstrated on DS1 is at the state-of-the-art (45 W/kg) and can easily be increased with now proven design enhancements and/or size increase. The specific power increases as wing size grows because the mechanism overhead of tie-downs and yoke diminish relative to the photovoltaic content. For example, with larger arrays the specific power approaches 70 W/kg for a 15 year GEO environment.

Generally speaking, *Scarlet* technology versus standard array technology is transparent to the spacecraft user, with one exception: pointing. DS1 has shown that the accuracy level required is not a significant engineering or operations burden. The required accuracy of the spacecraft knowledge and pointing was set at 0.5° maximum. Typically communications spacecraft point to better than 0.1° , so this was not a novel challenge.

However, if needed, the technology can also be configured for wider pointing acceptance angles. The optics are not sensitive to errors in one axis and thus GEO orbit seasonal off-pointing ($\pm 24^\circ$) can be accommodated with only a small reduction in performance.

3.4 Detailed Design Description

3.4.1 Overview

The basis of the technology is to use a linear refractive Fresnel lens to focus sunlight onto a 1 cm wide strip of solar cells as shown in Figure 4.

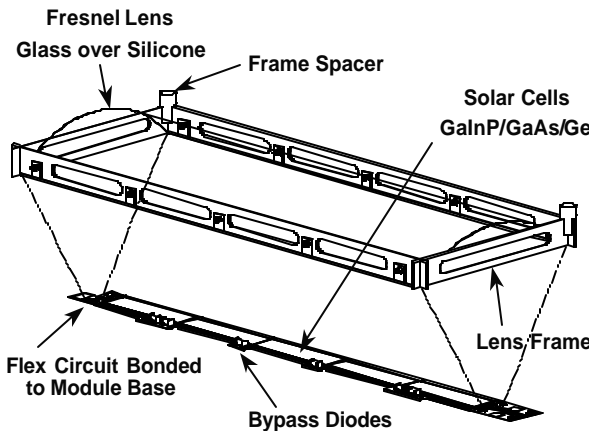


Figure 4. Scarlet Module: Lens and Receiver

The *Scarlet* array for DS1 is based on the prototype *Scarlet* array that was built for the METEOR satellite in 1995. [ref. 1] After the failure of the Conestoga launch vehicle, the BMDO Innovative Science and Technology Directorate sponsored the development of this second-generation *Scarlet* solar array - which incorporates advanced technologies such as multi-junction solar cells and an improved structural design - for use and validation on DS1.

The first generation *Scarlet* array was a melding of ABLE's standard planar array structure, PUMA [ref. 2], with concentrator optics. That structural baseline was reassessed for the DS1 *Scarlet* design to improve the union between the cell substrates and lens panels. The result is a simple cable-synchronized structure which deploys flat. The major advantages are fewer piece parts,

simplified pointing control analysis, reduced stowed volume, and simplified yoke structure. Additionally, the lens panels are held securely between power panels in the stowed condition.

Basic proven mechanisms such as release assemblies, tiedown cup-cones, cable pullers, and hinges of *Scarlet* I were utilized again for *Scarlet* II, but optimized to minimize weight. [ref. 2]

3.4.2 Mechanical Description

The DS1 *Scarlet* solar array consists of two wings of four panels each. The wings are delivered fully integrated with tiedowns, gimbal drive assembly, and spacecraft interface plate as shown below.

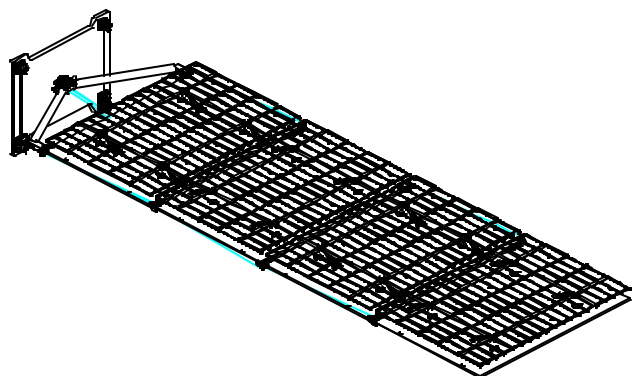


Figure 5. DS1 Scarlet Wing

Deployment of a wing is initiated when power is applied to the high output paraffin (HOP) linear actuators in each of two tiedown assemblies. A resistive load causes the paraffin to heat and change phase, which forces a pin forward releasing the restraint arm on a torsion tube. Tiedown cables are wrapped and captured in fittings on either end of the tube, so when a torsion spring revolves the tube, both cables are released. When the second release mechanism has actuated, the wing unfolds, driven by double-wound torsion springs distributed on each hingeline.

The hingelines are synchronized by a system of cables which are wound over static pulley cams. The synchronization transfers the deploy torque to the root where redundant rotary viscous dampers retard the deployment rate.

3.4.3 Electrical Description

The cells used by DS1 *Scarlet* are about 1 cm wide and 4 cm long and are spaced in rows 8.6 cm apart. The low cell area per watt needed beneath the concentrator greatly lowers cost and also eases the risk of utilizing emerging, high-performance cell technologies. For this reason,

BMDO elected to specify the procurement of an entirely multibandgap-cell-based solar array.

In 1996 production quantities of GaInP₂/GaAs/Ge dual-junction cells were not yet available. Tecstar was the only cell vendor willing to participate, and the DS1 team was cautious about the difficulties of bringing new cell technology into production. So to mitigate risk, and to set performance criteria for the flight build, an engineering build quantity of 100 cells was procured.

The III-V cell design, termed “Cascade” by Tecstar, had previously been qualified in the standard series of environments for space applications. The only modification required was gridline sizing for the high flux profiles of the concentrator.

The engineering evaluation result was very encouraging, with the average efficiency result coming in at 24.25% at 7.5X air mass zero (AM0). The performance criteria for the flight build was set at 23.25%, - partially because of losses anticipated for over-glassing, but mostly as insurance against the uncertainties of a larger build.

During the flight production phase Tecstar experienced a series of setbacks in producing the flight cells. The most persistent problem was shunting (Reviewed in [ref. 3]) which reduced the performance of many of the cells to as low as 16% at 1 sun intensity. Fortunately, the high current injection levels created by the lens overrides the fixed magnitude shunts and the performance at concentration is only slightly degraded.

After intensive effort by Tecstar, and aided by the synergism of the early dual-junction-cell manufacturing technology (ManTech) development program, remarkable improvement in yield and performance were achieved. But schedule delays eventually forced the acceptance of cells with a minimum lot average - under 7.5X concentration - of 22.6 %.

The cells were covered by Tecstar with 0.004-inch-thick coverglass with an anti-reflection coating with blue/red filtering (BRR). The reflection of the near infrared lowers the operating temperature of the cell by 11°C.

The cell receiver module consists of five series cells, each with bypass diodes, affixed to a circuit on a high thermal conductivity substrate as depicted in Figure 4. The modules are joined using overlapping redundant tabs with reflowed solder to form 50 cell strings that generate 40 watts at an operating voltage of 90 volts at 1 AU.

Cells in the module are interconnected along both their long edges. Given the long aspect ratio (4:1), the most probable crack direction will never leave a section of the cell isolated. Dual ohmics also provide balanced off-track performance and lower gridline resistance losses.

Cell interconnect reliability is also greatly improved over standard CIC construction because 120 interconnects (in parallel per cell) connect the cell to the circuit board carrier. The automated wire bonder, which stitches at a rate of three cells per minute, results in large cost savings by eliminating hand labor.

Engineering modules underwent thermal cycling from -160°C to +110°C for 100 cycles to assure a high margin of compatibility with the single thermal cycle experienced on the DS1 mission at the start of its interplanetary mission. All modules experienced no visible degradation and comparison of pre- and post-IV curves under the X25 solar simulator at NASA Glenn Research Center (GRC) showed no measurable electrical degradation.

To demonstrate the orbital applicability of the *Scarlet* technology, flight modules and lenses were later successfully cycled for GEO thermal extremes for 1350 cycles and to MEO extremes for 40,000 cycles.

3.4.4 Optical Description

The Fresnel lens is comprised of precisely formed individual ridges which refract incident light from a 3.22-inch aperture down to a strip of light focused in the middle of the 0.40-inch-wide cell strip to leave margin for pointing error.

The average optical efficiency of the DS1 lenses, which have no anti-reflective (AR) coatings, (used with the Cascade cell described above) has been measured at 89%. The effective concentration ratio, 7.14 (= 0.89 x 3.22/.40), was selected to provide for reasonable pointing error. The purpose was to create a cost-effective system to manufacture and assemble which is compatible with standard gimbal and spacecraft ACS architectures.

The linear Fresnel pattern is molded in a continuous roll process using space-grade silicone. Individual lenses are machined-trimmed and bonded to glass superstrates which have been thermally formed into cylindrical sections. The materials chosen for the lens, the bondline, and the glass are well understood: DC 93-500 silicone and ceria-doped borosilicate glass (Corning 0213). The glass protects the lens from particle radiation and with an AR/ITO (Indium Tin Oxide) coating, planned for future programs, the optical efficiency is enhanced and charge buildup is minimized.

The space between lenses must be minimized to maximize packing factor (the ratio of the area of light which passes through the lens to the total panel area). To demonstrate the survivability of the thin glass lens mounted in this minimal structure frame, five lens-in-frame components were tested - successfully - to conservative local acoustic/random levels (29 G_{ms} out-of-

plane, 9 in-plane). In qualification testing of the completed wings less than 2% of lenses had any cracking.

The efficiency of the lens overall is a function of the refractive index matching of the lens, superstrate, and optical coating used, as well as the surface finishes and sharpness of the lens teeth. The manufacturing of the lens produces smooth and sharp prisms with small root radii. The close match between the refractive index of the silicone and the glass (1.523 and 1.409 respectively) causes a slight loss of 0.3%. The losses are summarized in Table 1.

Well established optical coatings would reduce the large loss the lens outer surface transmittance, but the thermal forming of the lens superstrates occurs at a temperature which is higher than the survival temperature of typical coatings. Application of AR coatings to the curved surface of the glass superstrate was developed at OCLI, but not in time to coat all flight lenses.

Table 1. Optical Losses in Lens Assy
(without AR coating)

Component	Material	Interface Reflection	Absorptance Scattering
Space	Vacuum	4.5%	0.0%
Cover	Glass	0.3%	0.5%
Lens	Silicone	3.0%	3.1%
Space	Vacuum		0.0%
Totals		7.7%	3.6%
Combined Loss:		11.0%	(Multiplicative along light path)

Two coated lenses flew on the DS1 array in positions where their contribution to module efficiency could be measured and compared to non-coated lenses. The coating developed combined AR performance with electrical conductivity, using ITO to dissipate charge to the grounded lens frame structure. Component testing of the coated lenses demonstrated a 2% efficiency gain.

3.4.5 Thermal Design

The thermal design challenge is to spread the absorbed but unconverted solar energy (heat) from the cell modules out across the panel to engage the full area and high emissivity of the graphite panel to radiate efficiently. The cell, circuit layers, and panel were analyzed with a detailed finite difference model so that material choices and thicknesses could be optimized to reduce the cell temperature. The calculation results, for 1 AU illumination, are shown in Figure 6.

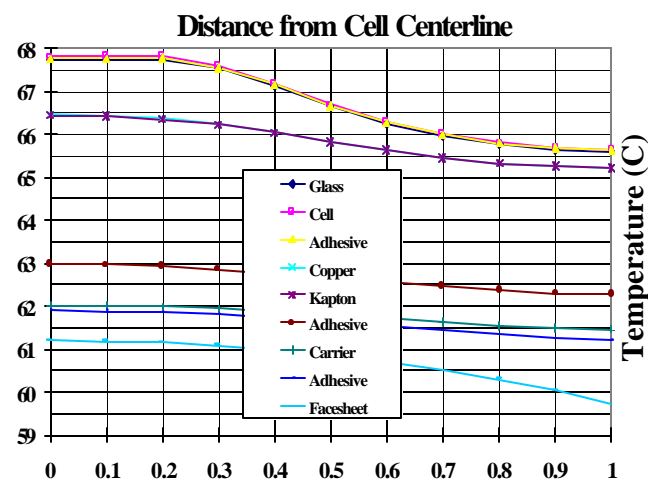


Figure 6. Temperature Profile Across Cell
(Edge at D = 1)

The largest temperature rise is caused by the Kapton. The thermally-conductive silicone adhesives and the cell carrier present very little resistance to thermal conduction. The carrier, which is used during cell laydown to stabilize the Kapton circuit and thus protect the cells from damage, is made of a high-conductivity composite to match the thermal expansion coefficient (nearly zero) of the panel. This creates minimal strain along the long bondline, and in addition, the material is very light and stiff.

As can be seen in Figure 7, once conducted to the panel the heat spreads rapidly out through the facesheets and core. This is because the facesheets are constructed of a ultra-high-conductivity fiber (which also possesses good compressive strength) which has a conductivity of 384 W/m-K (for unidirectional layup, 60% fiber volume), which is 60% higher than pure aluminum.

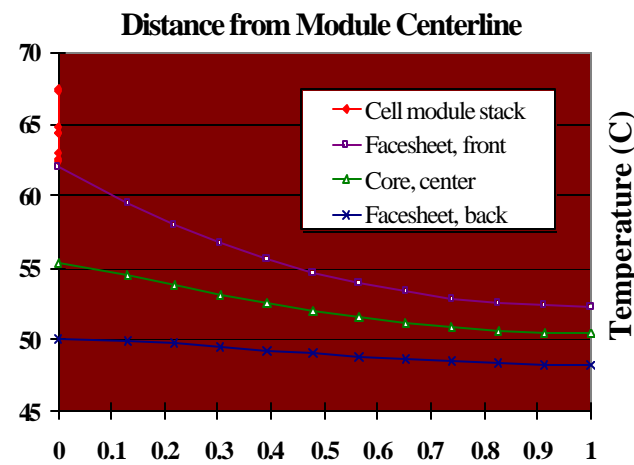


Figure 7. Temperature Profile Across Panel
(From cell center to centerline between module rows)

Typically, *Scarlet* cells operate about 20°C hotter than a planar GaAs design, mostly due to front surface radiation blockage by the lenses and the temperature gradients associated with heat spreading. The thermal modeling was first correlated to a balloon flight module [ref. 4] then later, with a vacuum thermal balance test at NASA GRC. The excellent agreement with the flight results, discussed later, was aided by these early validations.

3.5 Technology Interdependencies

The performance of many subsystems is often critical to the survival of a spacecraft. Of the dozen new technology experiment on DS1, several also functioned as bus subsystems. Perhaps the most critical to the mission is the power system - the *Scarlet* array. Without a functional solar array, a spacecraft cannot long survive. If the array had suffered even slightly degraded performance the ion engine may not have been able to thrust at a level sufficient to meet the first encounter target.

But the critical nature and unique features of the *Scarlet* array were generally transparent to the other spacecraft subsystems. It was mated to the spacecraft with no more interfaces or complexity than a generic solar array.

One important exception is that in operation the array requires much tighter pointing control than standard arrays. The pointing abilities of the spacecraft were not taxed by this need. The array included Moog-SMI gimbal assemblies with excellent orientation capability. The largest error sources were in the sub-assemblies of the wing itself. At one point in the mission a software, potentially a single event upset, caused one wing to off-point significantly. The inherent redundancy of the two wing system prevented the temporary power loss from threatening the mission.

3.6 Test Program

Due to limitations in evaluations that can be feasibly executed on-orbit, a thorough validation of technology such as *Scarlet* is highly dependant on ground testing. Of course, a systematic qualification test program is also essential to minimize flight risk. The ground test program (reviewed in detail in ref. 5) is discussed below as a prelude to the flight observations.

3.6.1 Ground Test Validation

Wing qualification testing was initiated once assembly of each wing was completed. No spare hardware was fabricated and a protoflight test approach on the flight hardware was used. The levels for the protoflight testing were defined by the DS1 Component Verification Specification (CVS).

Figure 8 shows the individual tests that were included in the program as well as the order that the tests were performed. Following each of the major tests (thermal cycle, acoustic, random vibration), the wing was deployed and inspected to verify that no critical damage occurred during the test. Before and after the full testing sequence, a full electrical functional test was performed on the wing to verify that the power level and electrical functionality of the wing was not degraded by the exposure to the test environments.

Deployment Tests: As part of the initial deployment tests, the array was deployed at thermal extremes, including a 10°C margin, based on modeling of the possible conditions in space at the time of deployment. The array was successfully deployed at -66°C, 30°C, and at ambient temperature.

Thermal Cycle Test: Thermal cycling was not a major issue for the DS1 mission because after the spacecraft leaves the earth's shadow following launch, it is in the sun for the rest of the mission. However, the CVS required a limited number of thermal cycles to ensure that the initial cycle from ambient (launch) to cold (umbra) to hot (in the sun) would not be a problem.

The wings were cycled three times between -123°C and +113°C. The temperatures were determined by mission analysis of the hottest and coldest possible conditions, plus margin. The tests were conducted in a dry nitrogen environment. Prior to array assembly, all of the flight array components had also gone through at least three thermal cycles.

Following the test, the arrays showed no measurable power reduction and no structural damage. Nearly 4% of the glass concentrator lens superstrates developed small cracks during the testing. However, the shape of the lens was maintained because the curved shape was formed in a zero stress state. The silicone adhesive also helped to maintain the configuration of the lens. No deformation or optical degradation was observed in the cracked lenses. All of the cracked lenses subsequently survived the acoustic and random vibration environments. Thus, the program decided not to replace the cracked lenses.

Acoustic Test: The wings were exposed to acoustic environments between 105 and 135-dB over a frequency range of 30 to 10,000 Hz during a 1-minute test. The arrays experienced no measurable power reduction or structural damage due to the test. As with the thermal cycle test, a small number of concentrator lens glass superstrates were cracked during the test, less than 2% of superstrates in this case. Again, there was no deformation or optical degradation and all of these lenses subsequently

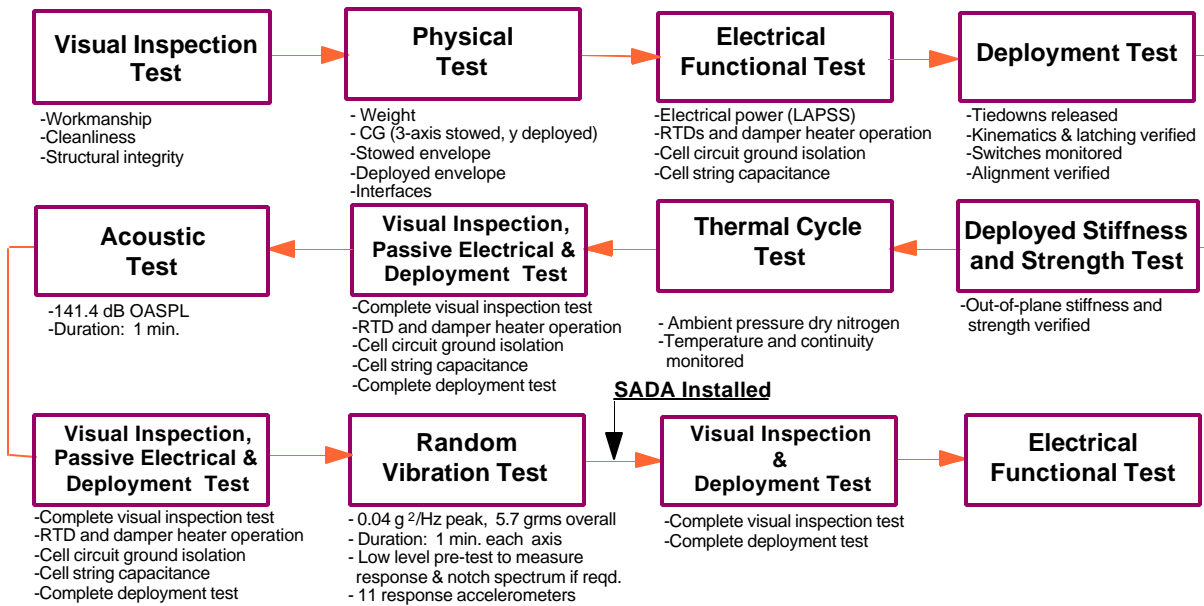


Figure 8. Protolight Test Sequence

survived the random vibration test. No other problems were observed during this test.

Random Vibration Test: The wings were random vibration tested in all three axes to the levels shown in Table 2. The test duration was one minute in each axis. As with the previous protolight test, the arrays experienced no measurable power reduction or structural damage due to the test. Again, a small number of concentrator lens glass substrates were cracked during the test; in this case, less than 1% of substrates. As in previous tests, there was no deformation or optical degradation.

Frequency (Hz)	PSD (g ² /Hz)
20	0.0016
50	0.04
500	0.04

Table 2. Random Vibration Test Levels

Power Measurement: The power was measured using a Large Area Pulse Solar Simulator (LAPSS). Due to the concentrator lenses, the light must be collimated perpendicular to the wing for the power to be measured. This required that wing power be measured one string at a time. The configuration of the strings results in an area of 17.3-cm across by 110-cm wide for each string. Testing showed that the light from the LAPSS was sufficiently collimated over this area. Special filtering was required to improve the LAPPS spectral balance for accurate multi-junction cell measurement (ref. 6).

All of the measurements performed as expected during these tests. Figure 9 shows the results of testing a string with and without the concentrator lenses. The string I_{sc} for a long series string was consistent with the measured average lens concentration ratio of 7.14. The string V_{oc} boost of 8% was consistent with individual module results. The string P_{max} increased by 4% more than expected (increased fill factor). This was determined to be due to the presence of shunts in some of the cells. Under concentration, the cells generate more current, so the shunts become less significant.

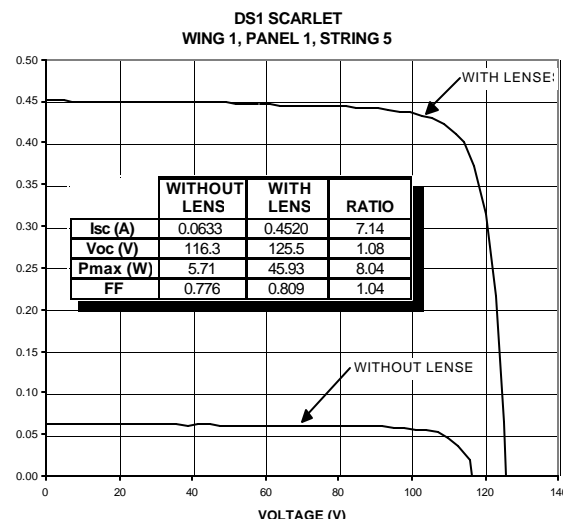


Figure 9. Scarlet String I-V Curves

3.6.2 Flight Test Validation

A large portion of the validation of *Scarlet* in flight was accomplished with the initial survival of the launch environment and successful deployment of the mechanism. After many months of data accumulation the power capabilities and robustness of the wing in the space environmental was convincingly demonstrated.

To reach our first goal at a 50% validation level, required the array - with its novel cable-linked synchronization, hinges, root articulation, four-bar lens panel kinematics, and latches - to perform as expected. 60% was obtained when the telemetry data was obtained and evaluated. A detailed review of the results is included in "Analysis of Flight Test Results, Deployment," Section 3.7.1.

Receiving the first power telemetry data set obtained 75% validation as even one data set gives flight confirmation of the capability of the technology to produce power in the space environment.

The original Power Telemetry data set was comprised of:

- Current and voltage (IV) curve data points for each of the 8 tap circuits
- Temperature readings from each of 10 RTDs
- Day, time, and heliocentric distance
- Wing orientations angles
- Spacecraft orientation reference data and wing angle null offsets

The information for wing and spacecraft orientation turned out to be superfluous. A measurement of the available power versus gimbal position was performed early in the mission as planned. The experiment demonstrated that the wings were so well aligned that power roll-off was not a factor. These results, which pushed successful validation past 80%, are discussed in "Analysis of Flight Test Results, Pointing," Section 3.7.2.

The operating temperature is a key element of the flight validation. The wings were well instrumented to measure cell temperature and gradients in the structure around the focal line. An analysis of the performance and a comparison to pre-flight expectations is discussed in "Analysis of Flight Test Results, Temperature," Section 3.7.3.

The sequence of commands executed by the spacecraft to collect and store the power telemetry data set is termed SIVPerf, for solar array IV performance. Because SIVPerf measures the IV curves of a single module within a string of 10 modules on each panel, whereon there are 9 strings, the calculation of total wing power production is a large extrapolation.

While the SIVPerf data is useful for certain investigations, there is another data set which gives much better confidence for full array power.

Successful execution of that sequence, termed SPeak for solar array peak power, affirmed the validation at 90%. Power production in excess of 2400 W. The various power telemetry from both SIVPerf and SPeak have been analyzed, combined, and contrasted to track the array power versus heliocentric distance and time.

The system power production has followed the original model very closely, thus completing 100% validation of the *Scarlet* technology in-flight, from mechanism structure and kinematics through thermal/optical/electrical modeling and power performance. The analyses of power performance are discussed in "Analysis of Flight Test Results, Power," Section 3.7.4.

3.7 Analysis of Flight Test Results

Analysis of the in-flight validation of *Scarlet* is grouped into four areas of performance: Deployment, pointing, temperature, and power. The following sections address the flight activities and data gathered and compare the data to pre-flight analyses and forecasts.

3.7.1 Deployment

The first activity required from the *Scarlet* system in space, deployment, occurred 1 hour after launch. The sequence plan for deployment of the wings was as follows:

0. Power to damper heaters (ON since launch)
1. Disable attitude control system (to prevent reaction during wing motion)
2. Power HOP primary heaters for 180 seconds
3. Power HOP secondary heaters for 180 seconds
4. Power HOP primary heaters for 180 seconds
5. Power HOP secondary heaters for 180 seconds

During steps 3-5, if all 8 release indications OR all 4 deployment indications become true, wait 10 sec then turn off the HOP heaters and go to step 6.

6. Wait 240 seconds for extension of wings ("deployment")

During steps 3-6, if all 4 deployment indications become true, turn off the damper heaters.

7. Turn OFF the damper heaters
8. Enable reaction control system
9. Index solar array gimbals

Through considerable discussion this conservative and straightforward algorithm was developed by JPL with ABLE input. In flight none of the redundancies proved necessary as the deployment was nominal. The logic of this sequence is as follows:

- Requiring all 8 tiedown release or all 4 deployment indications was to protect against a false positive, while still allowing quick re-enabling of attitude control and positioning of the array to the sun.
- Waiting 180 seconds before looking at the switch status meant that a primary heater failure could be tolerated too. This double failure protection was felt to be justified by JPL because of problems with microswitches in the past.
- Broken wires or open connectors can cause a false positive, because in all cases the microswitch configuration desired for positive indication was “open.” False negatives from the switches were prevented from being a detrimental factor, by OR-ing the tiedown set with the deployment set, and because the sequence would run regardless of microswitch problems.
- Waiting 10 seconds after getting all 8 release or 4 deployment indications was added to prevent any possibility of indications coming before actual release.

Activation of the paraffin actuators activates the mechanism to release the panel tiedown cables. After the tiedown cables are released, the wing deploys powered by torsion springs and rate-limited by viscous dampers. The nominal timing and range in protoquail testing for the release activation and the unfolding of the wing are shown in Table 3.

Table 3. Protoquail Deploy Timing Ranges

HOP Temp (°C)	Release Time (sec.)
30	60 ± 10
18	77 ± 7
0	110 ± 15
-10	130 ± 30

Power to the tiedown mechanisms was autonomously commanded at about 6:08 am PDT on October 24, 1 hour after launch. The spacecraft was in eclipse. Telemetry

was being recorded at 5-second intervals. Forty minutes later, when the real time link was reestablished at JPL and the monitors filled with data, it was evident the array was deployed: The indicator switch states were all in agreement and power was being produced.

Later analysis of the recorded data allowed the duration in seconds of the deployment events of HOP heating to SATM release and damped wing motion to latching at full deployment to be determined, as listed in Table 4.

Table 4. Flight Release and Deploy Durations

Event Duration	Time in	seconds
	Wing 1	Wing 2
I st Tiedown Release	75	70
2 nd Tiedown Release	85	80
Deployed & Latched	85	80
Total Time	170	160

The HOP heating durations on each of the four actuators ranged from 70 to 85 seconds. These values agree well with the duration predicted, 77 seconds, for the HOP temperature of 18°C. The thermal modeling of the temperature transients from fairing jettison after launch to deployment in eclipse is shown in Figure 10. The model predicted a HOP temperature of 15°C.

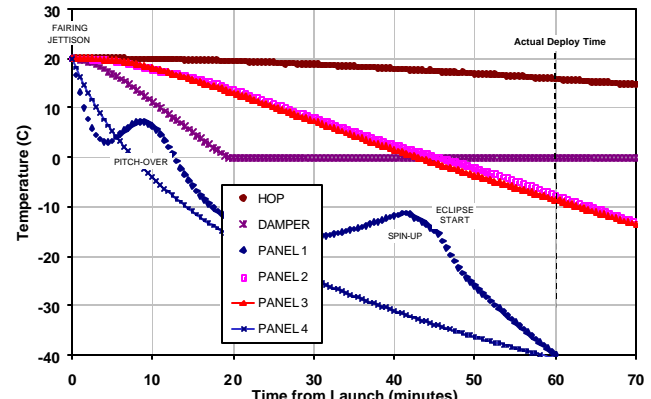


Figure 10. Ascent to Deployment Temp. Transient

The duration of the wing deployment depends on the damper temperature, which was forecast to be near zero. The damper body and silicone fluid and thermostat were modeled by a single node, as the primary intent was to determine how early the thermostat could turn on causing the damper heater to draw power and if the 10 watt heater was sufficient to maintain the damper above 0°C.

The actual fluid temperature would certainly lag behind the cooling of the casing exterior and the thermostat body.

So the flight temperature was probably between 0 and 15°C. Placing the average wing deployment time on the curve of predicted time versus temperature, Figure 11, suggests the fluid temperature was near 11°C.

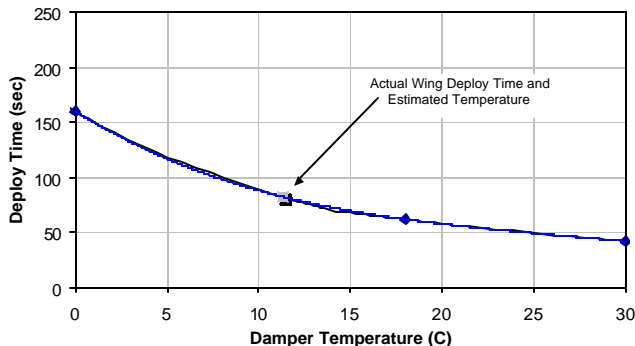


Figure 11. Deployment Duration vs. Temperature

In summary, all telemetry indicates the deployment occurred precisely as designed. This was a significant milestone for technology validation because - although the highlight of the technology is the optical/thermal/electrical performance of the concentrator/cell module - the kinematic control and joint mechanisms were also making their debut.

3.7.2 Pointing

The criticality of proper alignment of a concentrator system is plain. System performance is dependent on all elements (cells, modules, lens frames, panels, hinges, yoke,...) being assembled accurately, being deployed reliably, and being resistant to thermal distortion. Numerous industry efforts to build concentrator systems have failed at various stages prior to launch due to the inherent design and manufacturing difficulties. The industry has had limited success of late with low concentration ratios, for example the STEX trough concentrator at 2X. The *Scarlet* system is the first system on-orbit to provide significant concentration benefits.

The Fresnel optics provide an advantage in tolerance to shape error that reflective systems lack. This technology, when properly integrated at a 7X concentration level with ± 2 degree error tolerance, creates a system with significant cost and performance benefits.

While it was demonstrated that manufacture of the piece parts and assembly of *Scarlet* was straightforward, the proof of success - power production - required on orbit data. Would each and every lens be pointed accurately to the sun within the accumulated errors of piece part fabrication, sub-assembly, system assembly, thermal distortion, spacecraft knowledge and pointing control? The eighth day of the mission provided an opportunity to find out.

On-Orbit Calibration: The sequence was termed SCal, for solar array calibration. To determine if each wing was positioned by the spacecraft (for beta) and the wing gimbals (for alpha) at the angles which provided maximum power, the wings were steered to various positions over a range of ± 4 ° in alpha and ± 8 ° in beta. The alignment of the system was judged by the short circuit current (I_{sc}) output, a direct indication of the light flux on the cells, of the tap modules on each panel.

The sequence ran for about 6 hours, where each beta position was selected and the various alpha positions were steered through. The drift of the spacecraft causes some random variation in the current output results, but a parabolic curve fit, see example in Figure 12, can be used to estimate whether the alignment of a module is centered or offset.

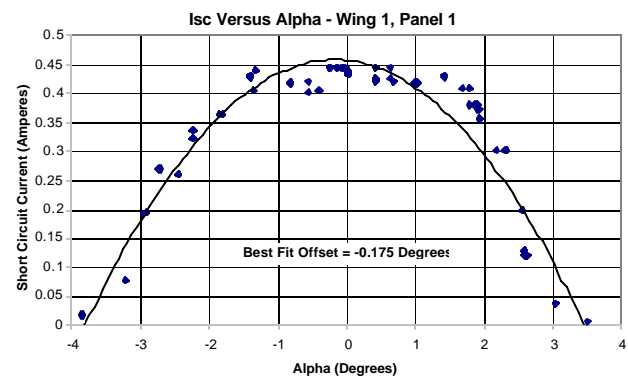


Figure 12. Light Collection versus Alpha Angle

When the offsets are compared against the design specifications, as in Figure 13, the success of the system in achieving far better alignment than required is clearly evident.

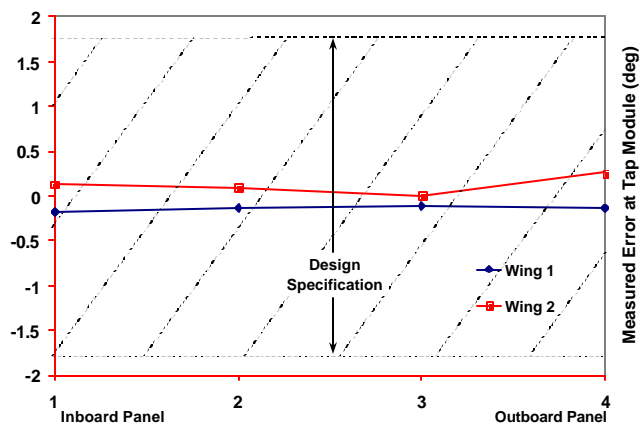


Figure 13. Pointing Validation Summary

In the event the SCAL data had shown any significant difference in current between modules or wings, a topology study was planned to determine the best beta correction for the spacecraft and the best alpha correction for each gimbal. Actually, it was hoped that an adjustment of pointing to achieve maximum power would not be required. Calibration is an activity that places a burden on spacecraft operations and it was important to demonstrate to future *Scarlet* users that it isn't required.

The results of SCAL demonstrated that *Scarlet* achieved the pointing accuracy goals not only for the design and assembly of the wings, but of integration with gimbals and the spacecraft structure, and for integrated performance with the spacecraft issues of position knowledge, pointing control, and drift.

3.7.3 Temperature

A critical validation of the power model is the operating temperature of the array. Each wing was equipped with resistance temperature devices (RTDs): Four on the inboard panel and four on the outboard panel. As shown in Figure 14, the cluster of four RTD's were located:

- Next to cell on the front facesheet (as close as Module Base width allowed)
- On module-to-module centerline on front facesheet
- Directly behind the cell on the back facesheet
- On module-to-module centerline on back facesheet

On the second wing only the RTDs nearest the cells were recorded, due to channel restrictions. Therefore the flight data set consists of 8 RTDs on Wing 1 and 2 on Wing 2.

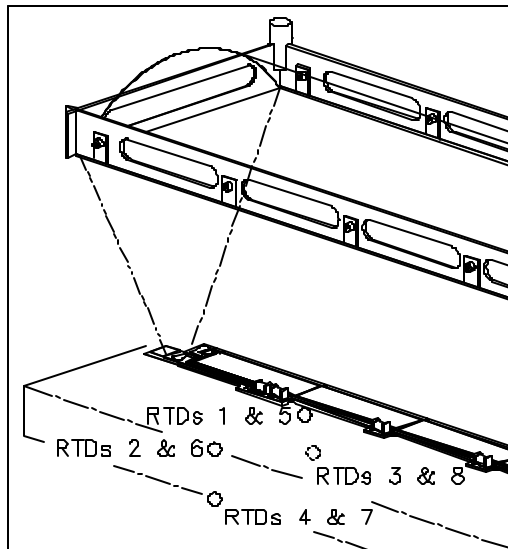


Figure 14. RTDs: 4 on a Module (in 2 Locations)

A fairly detailed finite difference model was developed, starting in 1996, to analyze the complex heat balance and thermal gradients beneath the lens. The line focus and regular module-to-module spacing allows for accurate temperature predictions using a half-symmetry 2-D model. The model was refined in 1997 based on thermal balance testing performed in a 1-sun vacuum environment at NASA Glenn Research Center.

The modeling results for each node of the model are shown in Figure 15, for the module at maximum power (minimum waste heat in cell). In this case the sun distance is set at 1.0174 AU, to correspond to the first applicable flight data set, presented next. The model is shown *without* the 10°C margin used in the power prediction, because the flight data demonstrates it was not needed, as will be shown below.

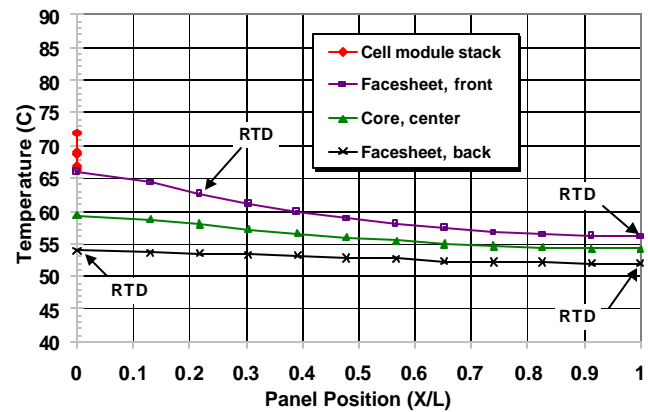


Figure 15. Thermal Modeling Results for 1.0174 AU

On the 37th day of the mission the ion engine was, for the first time, commanded to thrust at increasing increments up to maximum available power. The data available on all the RTDs at the intermediate levels between zero and near full power are plotted in Figure 16.

The model prediction curve is also plotted for comparison. The general agreement is excellent. Several observations about the data can be made:

- The agreement is fairly precise, on average, near maximum power for the RTDs nearest the cells.
- The flight data shows the gradients of heat spreading across and through the panel were slightly larger than the model forecast.

Since the gradients are larger than expected, but the near-cell RTD temperatures were accurate, it can be surmised that optimistic and conservative simplifications in the model were offsetting. Two known corrections which would reduce model conservatism are:

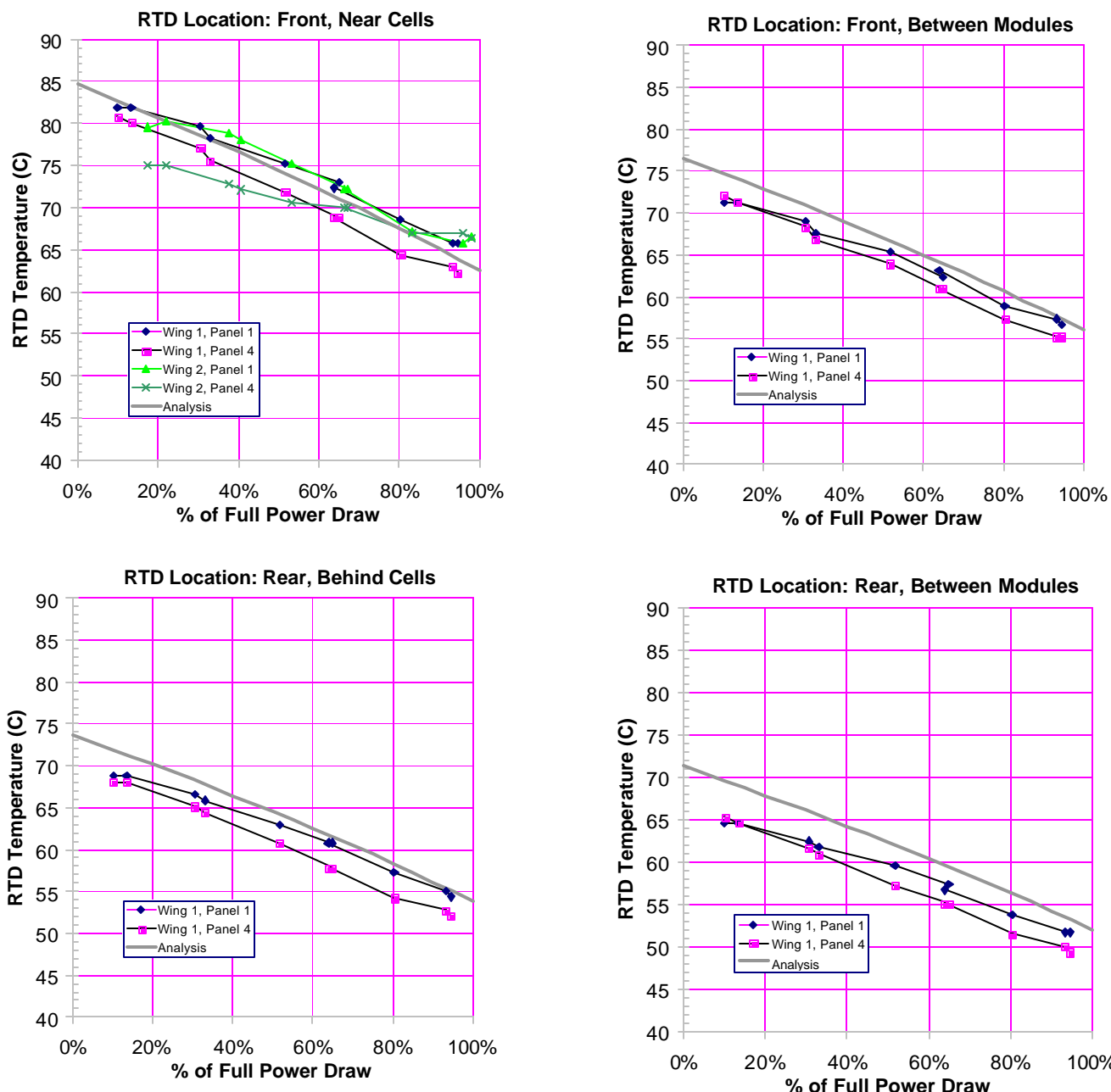


Figure 16. Steady State Temperature vs. Power Draw

- Recent analysis of the various optical filtering effects - both gray and wavelength dependent absorptance, scattering and reflectance - of the lens superstrate, silicone lens, cell cover, and cell have shown that the fraction of sunlight which reaches the cell is less than previously assumed.
- The carbon-carbon carrier beneath the cell is 50% wider than the cell, but this was conservatively not represented in the model.

The most likely effects which would reduce the efficiency of thermal spreading are: The core to facesheet conduction is limited by the joining adhesive, and/or the facesheet conductivity is lower due to thickness or resin fraction.

The net effect of incorporating corrections for these optimisms and conservatisms would likely be of little benefit to the power modeling correlation since the thermal modeling predicted the near-cell temperature precisely and is only off by 2.5°C on the back of the panel between modules.

3.7.4 Power

The validation of power production relies on two sequences: SIVPerf and SPeak, which stand for solar array IV performance and peak power, respectively. SIVPerf measures the full IV curve of a 5cell module within a string of 10 modules on each panel, for a total of eight module level curves. SPeak produces a partial IV curve for each wing, as a byproduct of a sequence intended to utilize the maximum power available for thrusting.

Because SIVPerf measures the IV curves of a single module within a string of 10 modules on each panel, whereon there are 9 strings, the calculation of total wing power production is a large extrapolation. SPeak is a better measurement of array performance and many more data sets have been collected leading to better correlating analysis and performance projections. The SIVPerf results will be discussed first.

SIVPerf: This validation sequence was run on the earliest day possible after launch using all tap circuits and temperature sensors (8 taps and 10 RTDs) to verify initial performance prior to on-orbit calibration. The first SIVPerf was run on mission day 7, October 31, 1998, the second on mission day 18, November 11, 1998.

The SIVPerf sequence was not run again until May 25, 1999. The 28-week testing hiatus was necessary to identify and correct a power distribution unit failure mode using software, upload and verify the new software, and to schedule the activity into the busy validation/operations planning.

The SIVPerf sequence provides certain types of data the SPeak test cannot. Namely, data to the left of peak power on the IV curve. The short circuit current is of particular interest as it validates the lens optical efficiency and functions as a monitor of the combined effects of UV and radiation darkening, outgassing contamination, and micrometeoroids.

The I_{sc} values for the modules shows significant change over time as the spacecraft has traveled out to 1.3 AU. For purposes of comparison the data, shown in Figure 17, has been corrected for insolation changes due to heliocentric distance and the effect of temperature as the cooling of nearly 50°C produces a significant current reduction.

The average of the early data shows that no significant darkening took place in the initial weeks on orbit. However, contamination of the lenses from spacecraft (or array) outgassing may have occurred prior to the first readings.

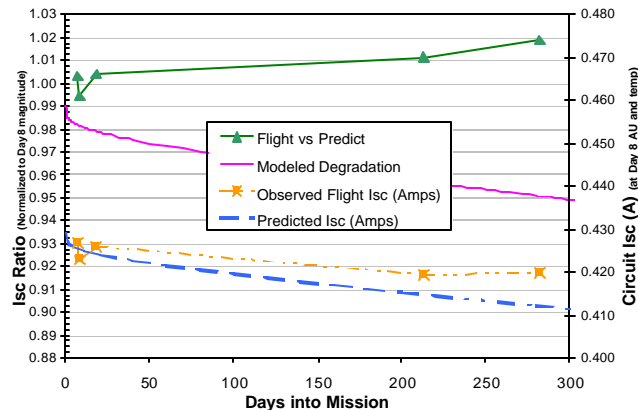


Figure 17. Short Circuit Current Degradation

The initial indications were that the sensitivity to short term UV was small as expected. The longer-term effects of UV darkening and radiation darkening are less than expected. The trend says the degradations over time have not been as severe as expected, indicating that the expected values for all or most of the degradation factors (S/C outgassing, optical losses in lens from UV degradation, UV degradation of cell/cover, and cell radiation degradation) were conservative.

It was the intent to be conservative in each of these factors. For example UV light is refracted over the cell coverglass. Degradation of the cover adhesive would only occur during times of off-pointing.

The radiation degradation was based on an analysis by the Aerospace Corporation performed in August of 1997. The EOL degradation was forecast to be 0.965. A linear degradation with time was assumed although actual degradation from constant fluence follows a high order polynomial. In truth, a large solar flare could occur at any point in the mission. Use of a linear fit compensates partially for the possibility of a large solar flare early in the mission.

Since the October 1998 launch solar sunspot activity has been well below historical averages, as can be seen in Figure 18, below. Since flare activity and particle radiation have been correlated to sunspot activity it is plausible that the radiation degradation is proceeding at well below the modeled rate.

It also is possible that the some other factor in the model was conservative or the data itself is optimistic (meaning actually lower) due to systematic inaccuracies.

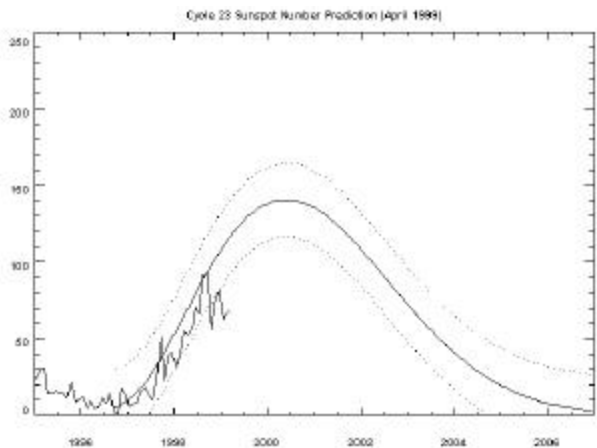


Figure 18. Historical Sunspot Activity

The entire IV curves for the eight modules showed no surprises. In general, the power output is much lower due to greater sun distance for the later two curves. Between day 213 and 282 the spacecraft traveled from 1.330 AU to 1.341 AU and back to 1.325 AU again. So the insolation level was essentially equal - as are the IV curves recorded - although 69 days have passed. The degradation of the lens appears smaller than is measurable.

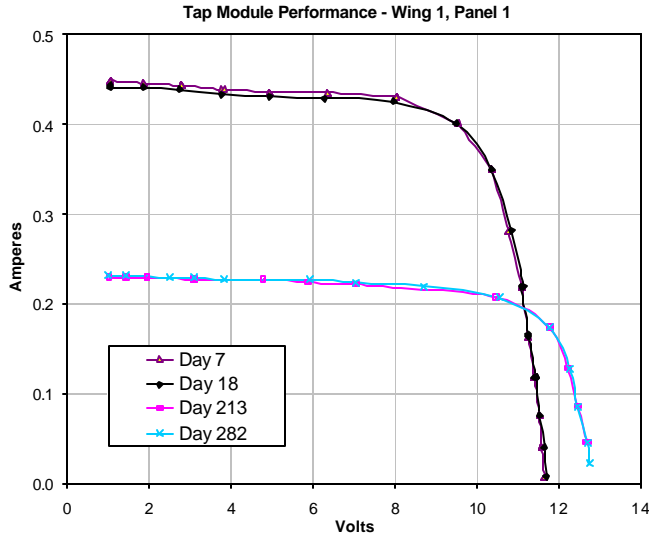
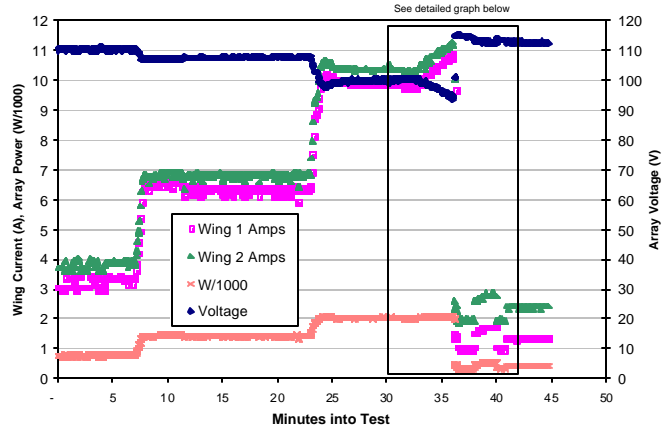


Figure 19. Tap Module - Wing 1, Panel 1

SPeak: The spacecraft electrical power system was designed with the capability to utilize the batteries as a buffer to allow maximum thruster output without collapse. A software routine, termed SPeak, finds the solar array peak power for use as an input to controlling operation at a maximized thrusting level. This routine provides the best information on array level performance.

The first SPeak sequence, on mission day 90, began by incrementally increasing the ion engine power level,

stopping at two intermediate points between nominal bus loads and maximum power, as shown in Figure 20. This was done to allow intermediate power level data to be recorded and to let the array cool to near the full power



operating temperature before moving to the full power load voltage.

Figure 20. SPeak Sequence Flight Data

The last setting was chosen to be about 100 W in excess of the expected maximum (preflight) predicted power of the array. The battery was relied upon to supply the differential power. The spacecraft software will step down the thrust level if the battery discharge exceeds a predetermined level.

During this test run, the load voltage set point was intentionally stepped lower at 0.3 V increments to obtain the most detailed data. As can be seen in the closeup of the data near max power, Figure 21, when the array peak power was approached, the increments of voltage resulted in negligible array power output change.

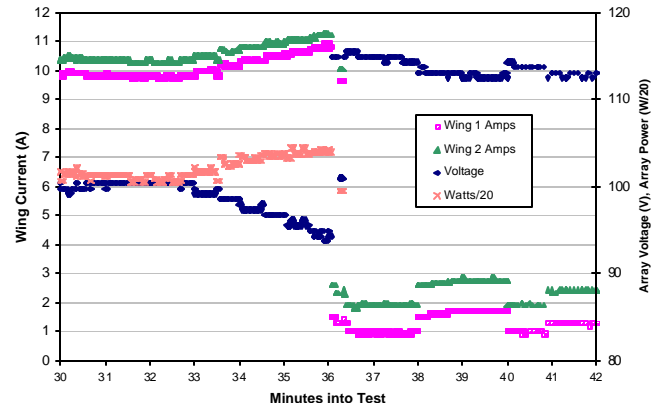
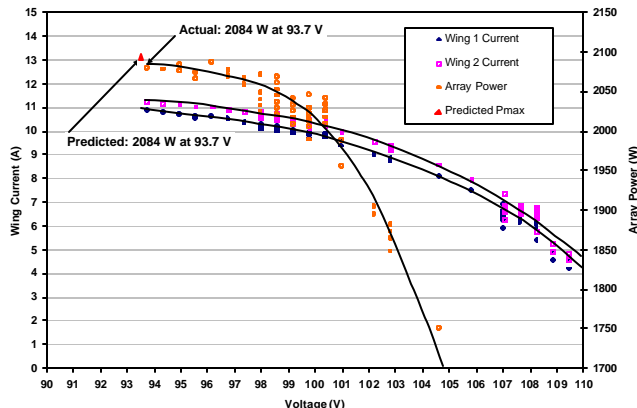


Figure 21. SPeak Sequence, Incrementing Voltage Near Peak Power

Plotting the wing currents against voltage rather than time, yields the more familiar "IV" curve. A detail of the data near the knee is shown in Figure 22.

**Figure 22. SPeak Data, Array Output at 1.1185 AU**

The power output has leveled off mostly, to 2084 watts, as the voltage was reduced to the last recorded value of 93.7 V. The flight values from the best fit curve are compared to the model predictions in Table 5.

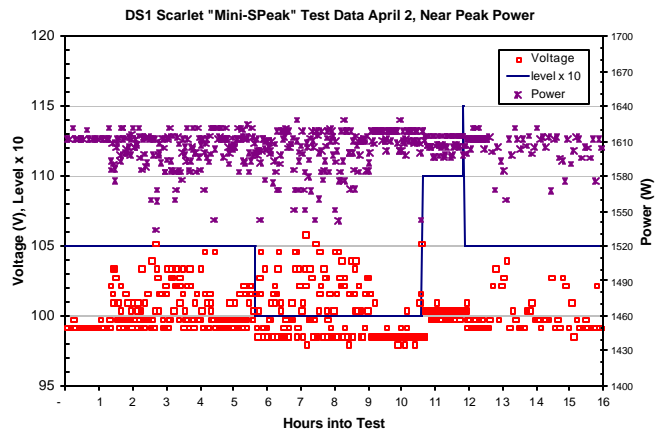
Table 5. SPeak Results Comparison

Value	V_{MP}	P_{MAX}
Prediction	93.5	2094
Flight Results	93.7	2084
FR/P Ratio	1.003	0.995

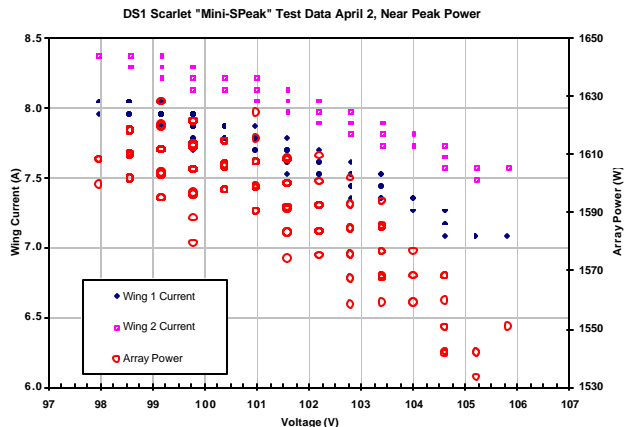
The excellent agreement between the forecast and the first flight results is a clear validation of the *Scarlet* technology.

The full SPeak test was found to be too time-consuming and a shorter version evolved, termed mini-SPeak. Three mini-Speaks were performed in April of 1999 on the 2nd, 8th, and 22th. During each test run, the load voltage set point was stepped at 0.6 V increments and held for a number of hours to record a significant number of data points at a low data rate. An example of the data set is shown in Figure 23.

No.	Date	AU	Predicted Power (W)	Predicted Voltage (V_{max})	Observed Power (W)	Observed Voltage (V_{max})
1	2-Apr-99	1.2676	1677	97.7	1628	99.16
2	8-Apr-99	1.2774	1653	98.0	1595	99.16
3	22-Apr-99	1.2978	1604	98.4	1538	99.76

**Figure 23. Mini-SPeak 1, Mission Day 160**

Plotting the wing currents against voltage rather than time, puts the data into the more familiar "IV" curve presentation. In Figure 24 is the IV curve near the knee as this is the point of interest (and the limit of the data set).

**Figure 24. Mini-SPeak 1, Peak IV Data**

The flight values for P_{max} and the associated voltage, determined from graphs like the previous example, are compared to the model predictions in Table 6.

Table 5. Mini-SPeak Results Comparison

A summary depiction of the flight data against the forecasts for power, peak power voltage, and temperature is shown in Figure 25. The flight data is summarized by month in charts in Appendix B. Hourly data is depicted for voltage, wing currents, and RTD temperatures (averaged for each of the four positions in module).

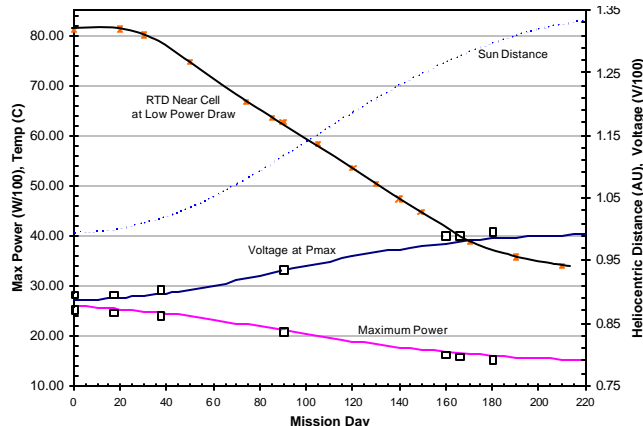


Figure 25. Original Forecasts and Flight Data

4. TECHNOLOGY VALIDATION SUMMARY

On DS1, the first mission of NASA's New Millennium Program, the *Scarlet* array has provided power as designed, over 2.5-kW at nominally 90 volts, to power the NSTAR ion propulsion engine, plus spacecraft bus loads, on the interplanetary mission.

The accomplishments of the entire DS1 *Scarlet* program, in summary, were:

- Development, manufacture and successful spacecraft integration of a novel advanced, multi-junction-cell-based, high voltage concentrator solar array;
- Flight validation of new structural, mechanical, optical and electrical systems;
- Flight validation of the modeling and predictions for power output;
- Successful operation of the concentrator system on the DS1 spacecraft.

These accomplishments were achieved over 3 phases: Pre-flight: design, fabrication, test and integration, Launch and initial deployment, and the initial cruise phase of the mission. The specific successes of the *Scarlet* technology achieved on DS1 were:

- Demonstration of novel technology

- ✓ The first successful concentrator array system in space
- Utilizing the most advanced solar cell technology
 - ✓ The first successful array system in space to use dual and triple junction solar cells
- Demonstrating high specific power
 - ✓ The first successful array system in space to use dual and triple junction solar cells
- Demonstrating structural robustness
 - ✓ The system stowed and deployed stiffness performance is excellent
- Being designed for producibility
 - ✓ This will allow for low recurring cost on future applications
- Supporting all DS1 mission requirements
 - ✓ The array performance provided the power needed to reach the encounter targets

The risks that are inherent in the creation of such new technology are numerous and complex. A large portion of risk retirement was completed with thorough ground tests, but many elements of the technology simply couldn't be validated without the success of the launch, deployment, and the subsequent flight operations performed by JPL. The areas of highest remaining risk prior to launch were:

- **Structural or electrical damage during launch**
 - Broken lenses, loose wires or cracked cells
 - Insufficient tiedown preload
- **Deploying successfully in zero gravity**
 - Imbalance from thermal loading
 - Cable loads*
 - Hingeline binding*
 - Mechanism torque margin
 - Array jump-out loading
 - Damper failure due to deadband
 - Panel insert strength margin
 - Failure of the lens frame to deploy
- **Proper alignment to the sun**
 - Shifts in mountings from launch loads
 - SC to array mounting accuracy
 - Gimbal pointing accuracy
 - Hinge stop adjustment
 - Thermal warping
 - Warping of the power panels and/or lens panels*
 - Moisture outgas shape change in composites
 - Alignment of module elements
 - Cells on carrier, carrier on substrate*
 - Lens panel over substrate*

Lens to lens spacing, lens shape

- **Providing power as expected**

AMO vs. LAPSS performance

Spectrum and collimation

Failed circuits

Mechanical failure

ESD induced failure

Operating temperature

Panel conductivity

Radiation exchange

Lens absorption and transmission

Environmental degradation

Particle radiation darkening of the lenses

UV radiation darkening of the lenses

Contamination from the ion engine or SC

Combined effects

Performance vs. AU

Temperature change

Insolation effects

While the telemetry for critical metrics such as power, temperature, deploy time, etc were documented to be as predicted, many of the risks listed above were impossible to cost-effectively monitor. From the proper performance of the system on mission the elimination of all these risks can be safely inferred.

The flight validation of *Scarlet* will allow a multitude of future users, particularly deep space science missions, mid-level orbit satellite applications, and communication constellations, to confidently baseline ABLE's product offering and garner the benefits of state of the art performance at a fraction of the cost of standard technology.

5. APPLICATION FOR FUTURE MISSIONS

The hardware demonstrated on DS1 is not the limit of this technology's promise. During the design and fabrication of the DS1 *Scarlet* array there was a concurrent review for potential improvements. A number of advancements were developed as part of ABLE's internal R&D effort. The most significant improvements which have been demonstrated to date are the elimination of the carrier used in cell laydown and of the lens clip stampings used in the lens panel assemblies. These improvements contribute equally to a 10% increase in specific power while reducing fabrication costs.

Additionally, a demonstration model has been built which shows the stowed height can be significantly reduced by nesting the lens panels into the substrate panels.

A common mission requirement, not required by the DS1 mission, is extended thermal cycling. The element of the hardware, peculiar to *Scarlet*, which is vulnerable to

thermal cycling stress - the lenses - was thermal cycled from -180 to + 110°C for a number of cycles equivalent to a 15-year GEO mission and from -160 to + 110°C for 40,000 cycles to represent a LEO mission.

NASA and BMDO also continue to develop technologies that will radically improve the performance of *Scarlet*. For example, the future development of advanced multiple band gap cells that will deliver 30 to 35% efficiency under concentration. Small cell size and low total PV area allow *Scarlet* to take advantage of such cells early in their production cycle when quantities are low and cost is high.

In addition, monolithic polymer concentrator lens materials that can survive both radiation and UV exposure are being demonstrated by an Entech/ABLE team. This will allow construction of much lighter foldable lenses and will lead to a huge gain in specific power and reduction of stowed volume.

For future applications the cost and performance advantages of *Scarlet* will be maximized for missions with high radiation or LILT conditions. As new exotic cells start to become available that promise large efficiency gains, but come with high initial production costs, the *Scarlet* technology can be effectively utilized. With a small size cell and a low total PV area a high power *Scarlet* array can be assembled.

6. ACKNOWLEDGMENTS

The triumph of DS1 and the *Scarlet* technology honors the efforts of dedicated engineers and technicians who produced a working system out of many novel technologies. Patience and commitment to problem solving of the team members at ABLE, BMDO, and JPL were all critical to the achievement. The effort to design and develop the *Scarlet* technology as described in this paper was performed under the sponsorship of the Ballistic Missile Defense Organization. Contributions by the Jet Propulsion Laboratory and the National Aeronautics and Space Administration were essential in mitigating risk and thereby producing a successful mission.

7. REFERENCES

1. Allen, D., Jones, P., Murphy, D., and Piszcior, M., "The SCARLET Light Concentrating Solar Array," Conference Record of the Twenty Fifth IEEE Photovoltaic Specialists Conference, IEEE, 1996.
2. Wachholz, J., and Murphy, D., "SCARLET I: Mechanization Solutions for Deployable Concentrator

Optics Integrated with Rigid Array Technology," Proceedings of the Aerospace Mechanisms Conf., 1996.

3. Eskenazi, M., Murphy, D., Ralph, G., and Yoo, H., "Testing of Dual Junction SCARLET Modules and Cells Plus Lessons Learned," Conference Record of the Twenty Sixth IEEE Photovoltaic Specialists Conf., IEEE 1998.

4. Eskenazi, M., Murphy, D., Anspaugh, B., Brinker, D., and O'Neill, M., "Balloon and Lear Jet Testing of SCARLET Modules and Cells," Proceedings of the 15th Space Photovoltaic Research and Technology Conference (SPRAT XV), 1997.

5. Allen, Douglas M., and David M. Murphy, "An Update on the Deep Space 1 Power System: SCARLET Integration and Test Results", 33rd IECEC Proceedings, Colorado Springs, CO, 2-6 August 1998, IECEC-98-403.

6. Krut, Dimitri D., Lovelady, James N., and Cavicchi, B. Terence, "Spectrally Balanced Light IV Testing of Production Dual Junction Space Cells", 2nd World Conference and Exhibition on Photovoltaic Solar Energy Conversion, Vienna, Austria, 6-10 July 1998.

Appendix A

In the table below is shown the telemetry channels for each of the two technology validation activities conducted on the spacecraft for *Scarlet*. The sequence SIVPerf characterizes the IV curves of 8 individual modules on the array. The sequence SPeak characterizes the peak power point of the array by stepping down the solar array regulation voltage setpoint while the ion engine is thrusting at a level high enough to induce array regulation.

Channel	Mnemonic	SIVPerf	SPeak
P-2030	SA_V	X	X
P-2040	SA1_I	X	X
P-2050	SA2_I	X	X
P-2061	ESS_BUS_V		X
P-2060	ESS_BUS_I		X
P-2062	NON_BUS1_I		X
P-2063	NON_BUS1S_I		X
P-2064	NON_BUS2_I		X
P-2065	NON_BUSS_I		X
P-2011	BAT1_I		X
P-2021	BAT2_I		X
P-3170	SA_MOD_LDSEL	X	
P-3171	SA_MOD_SEL	X	
P-3172	ARR_OPV_SL_C		X
P-0020	BAT1_SOC		X
P-0022	BAT2_SOC		X
P-4041	SA1_VAL_TMP1	X	X
P-4042	SA1_VAL_TMP2	X	X
P-4043	SA1_VAL_TMP3	X	X
P-4044	SA1_VAL_TMP4	X	X
P-4045	SA1_VAL_TMP5	X	X
P-4046	SA1_VAL_TMP6	X	X
P-4047	SA1_VAL_TMP7	X	X
P-4048	SA1_VAL_TMP8	X	X
P-4051	SA2_VAL_TMP1	X	X
P-4052	SA2_VAL_TMP2	X	X
P-2031	SA_MOD_I_TLM	X	X
P-2032	SA_MOD_V_TLM	X	X
P-3081	SA_MOD_I	X	X
P-3082	SA_MOD_V	X	X
P-3170	SA_MOD_LDSEL	X	X
P-3171	SA_MOD_SEL	X	X
B-3101	SA_OP_PT LSB		X
P-0006	ARR_OPV_SEL		X
B-2082	HCDCRC0_STA		X
V-0141	XLINECUR		X
V-0142	XLINEVOL		X
V-3421	XTHRTLVL		X
V-3421	XTHRTLVL	X	
A-1401	ACMSUNBODY0	X	
A-1402	ACMSUNBODY1	X	
A-1403	ACMSUNBODY2	X	
A-1711	SADA_ANGLE_0	X	
A-1712	SADA_ANGLE_1	X	

APPENDIX B

Table B-1. Array Validation Activities Timeline

Mission Day	Activity	Date	DOY
7	SIV Perf Seq	31-Oct-98	304
8	SCal Seq	1-Nov-98	305
18	SIV Perf Seq	11-Nov-98	315
90	SPeak Seq	22-Jan-99	022
160	Mini SPeak	2-Apr-99	091
166	Mini SPeak	8-Apr-99	098
180	Mini SPeak	22-Apr-99	121
213	SIV Perf Seq	25-May-99	145
279	Mini SPeak	30-Jul-99	211
282	SIV Perf Seq	2-Aug-99	214
285	Mini SPeak	5-Aug-99	217
285	Mini SPeak	6-Aug-99	218
325	Mini SPeak	14-Aug-99	257
346	Mini SPeak	5-Oct-99	278

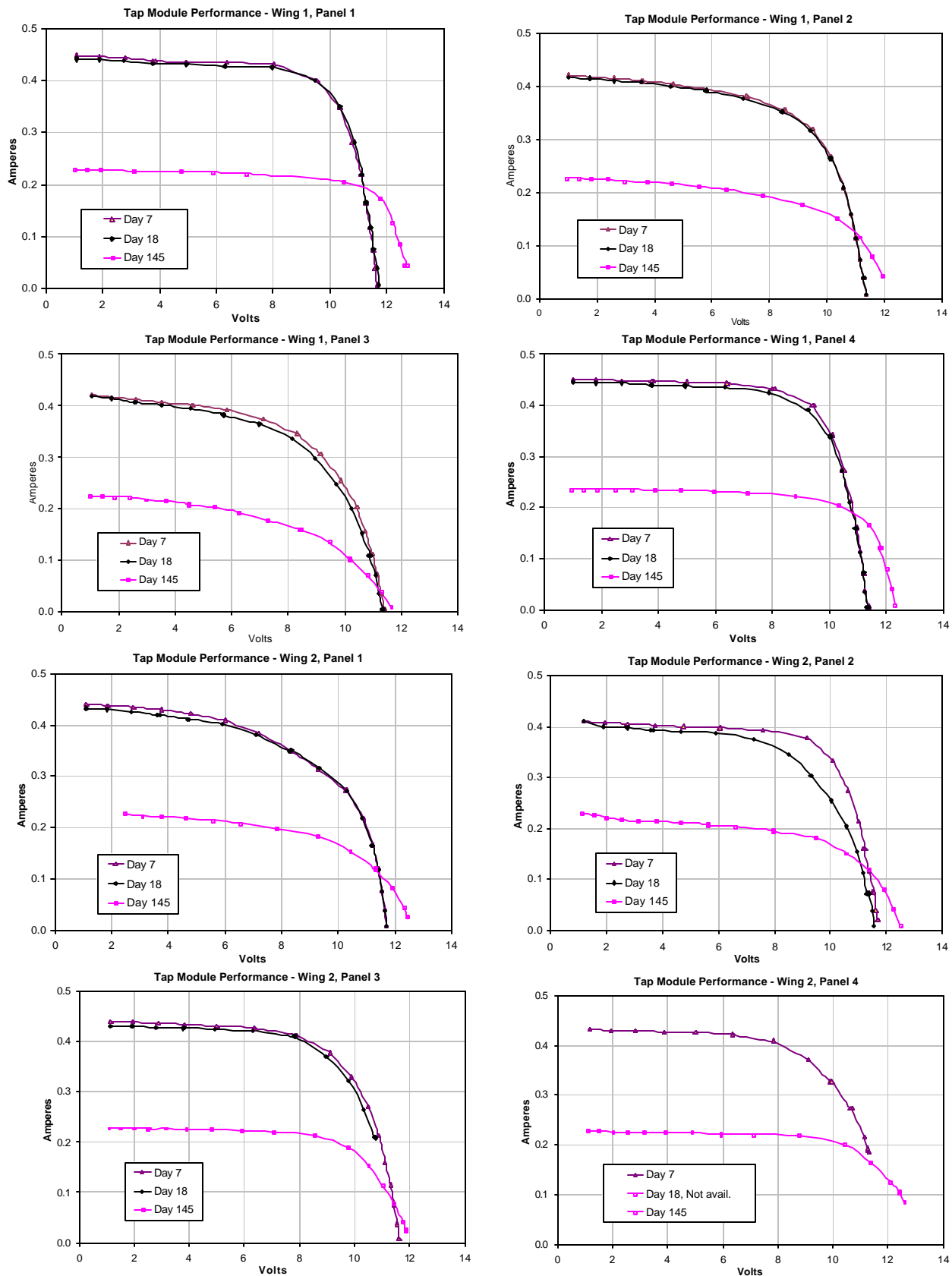


Figure B-1. SIVPerf Tap Module Data for Mission Days 7, 18 and 213 (DOY 145)

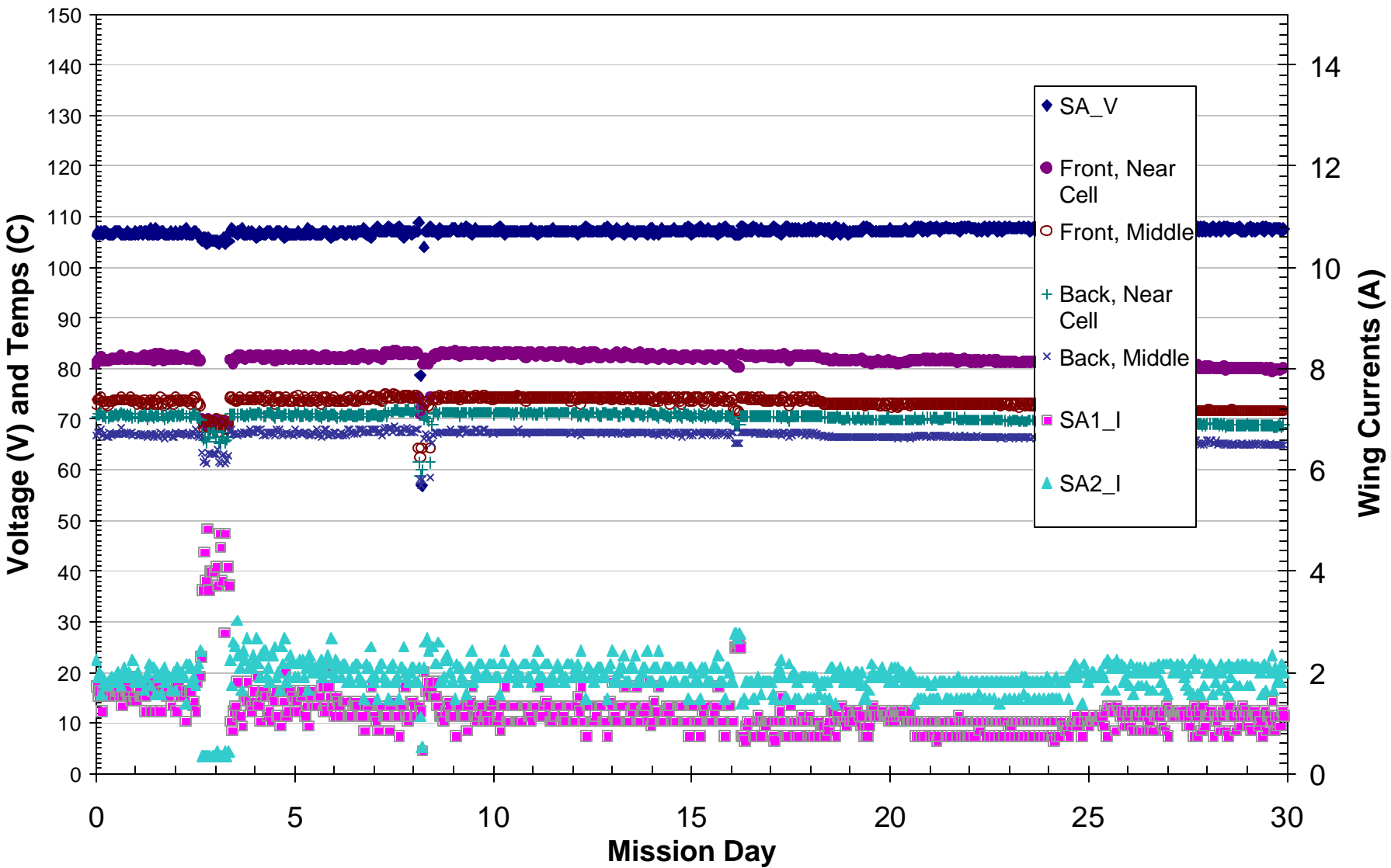


Figure B-2. DS1 SCARLET Array Data Hourly: First Month of Mission

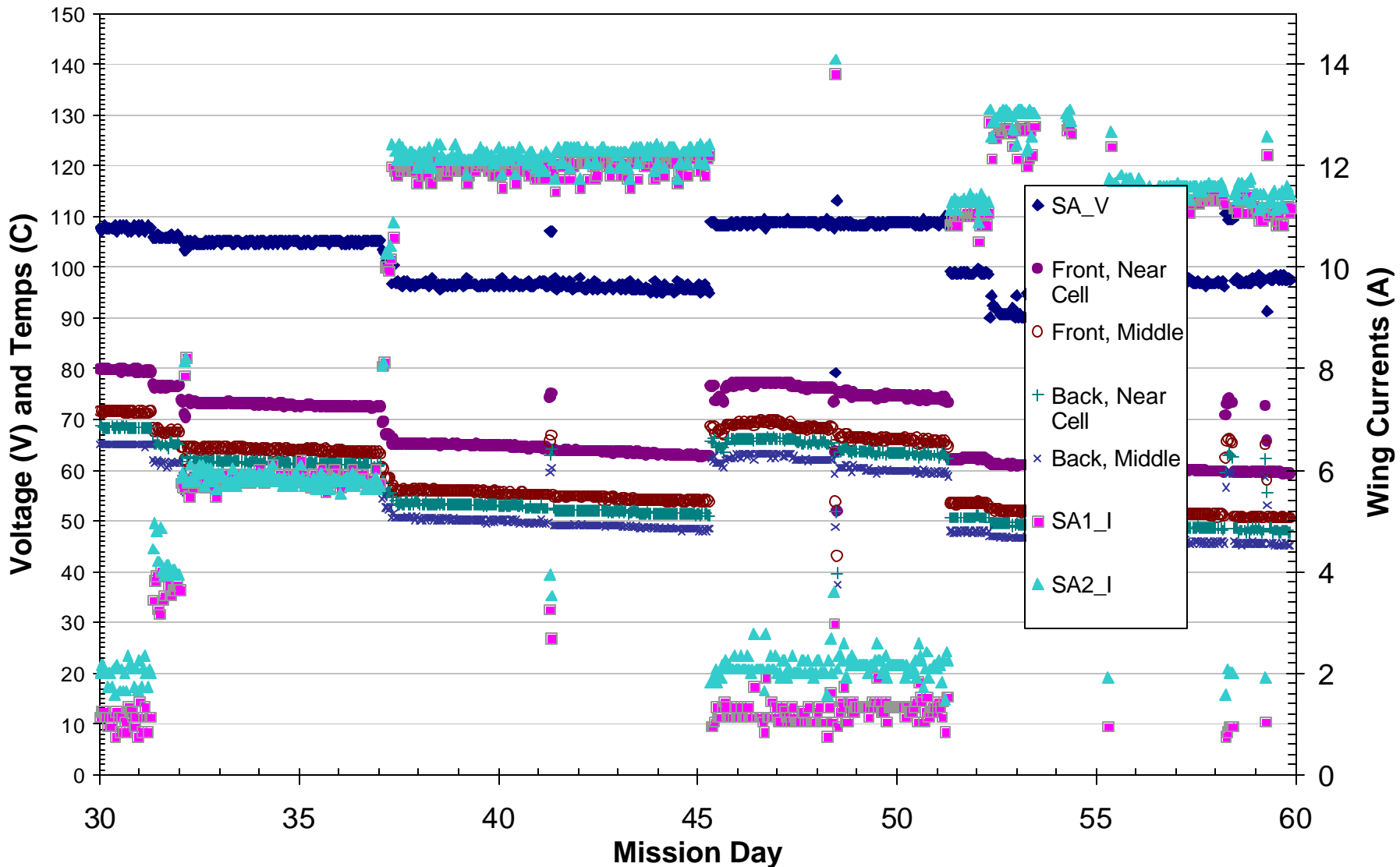


Figure B-3. DS1 SCARLET Array Data Hourly: Second Month of Mission

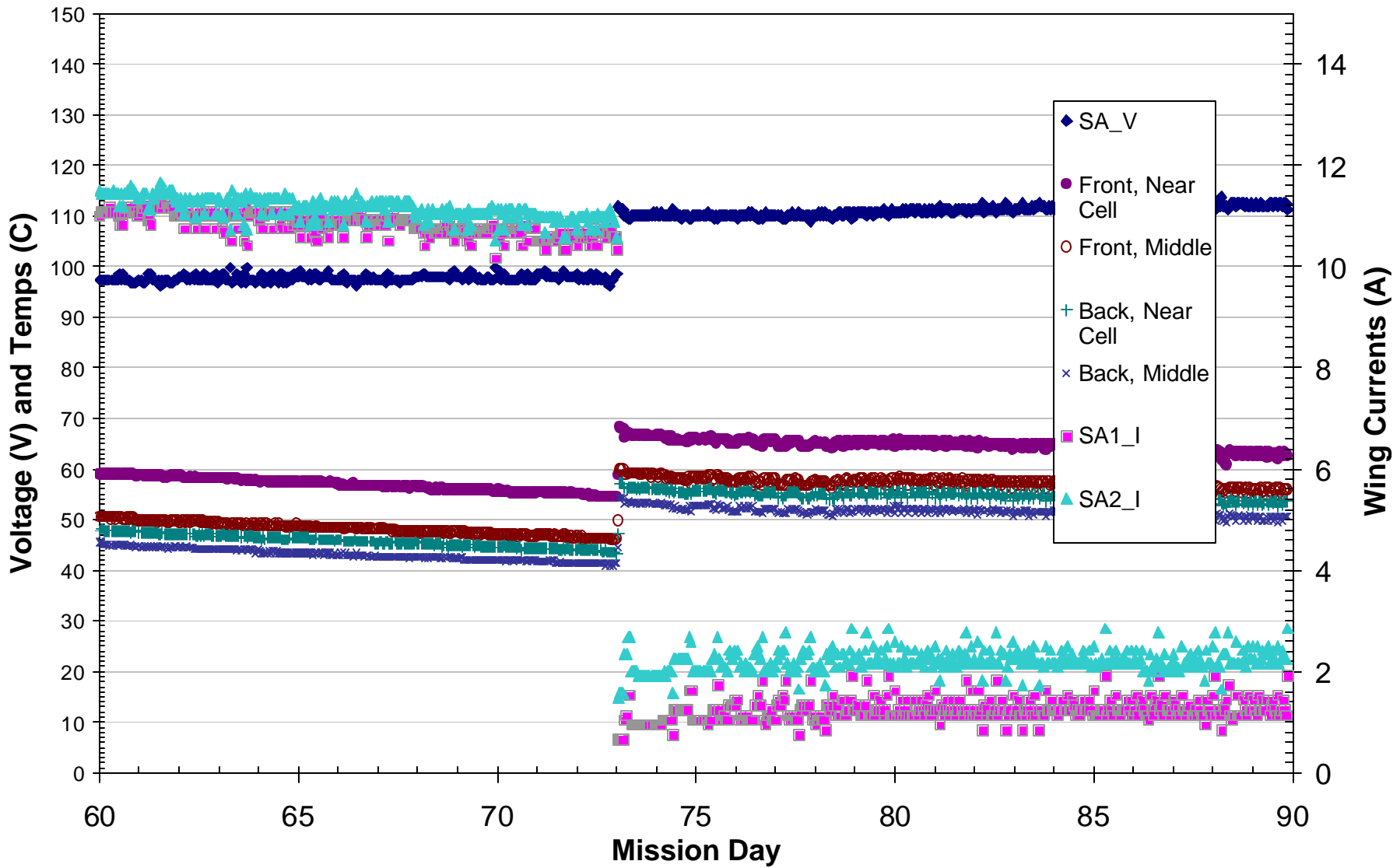


Figure B-4. DS1 SCARLET Array Data Hourly: Third Month of Mission

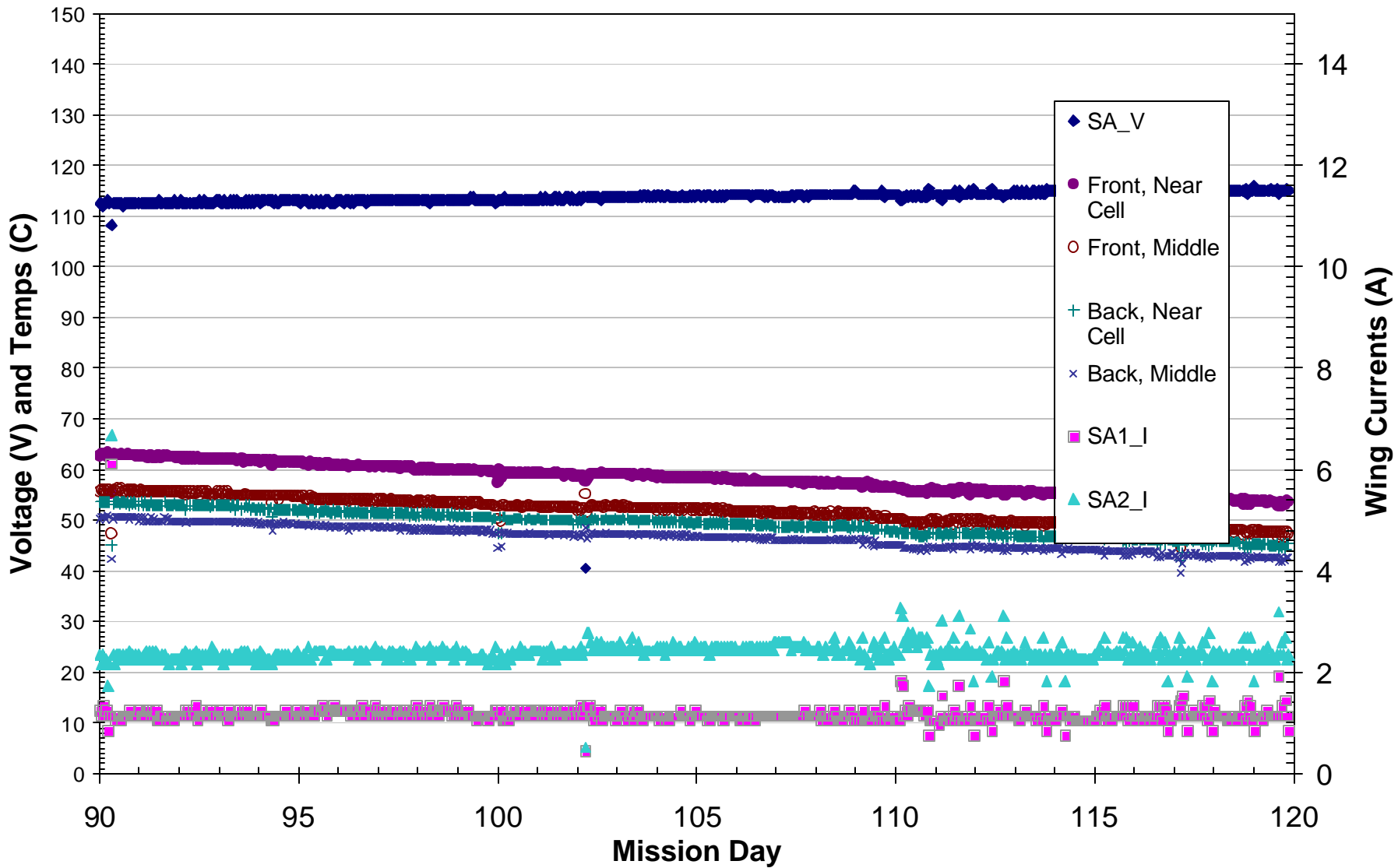


Figure B-5. DS1 SCARLET Array Data Hourly: Fourth Month of Mission

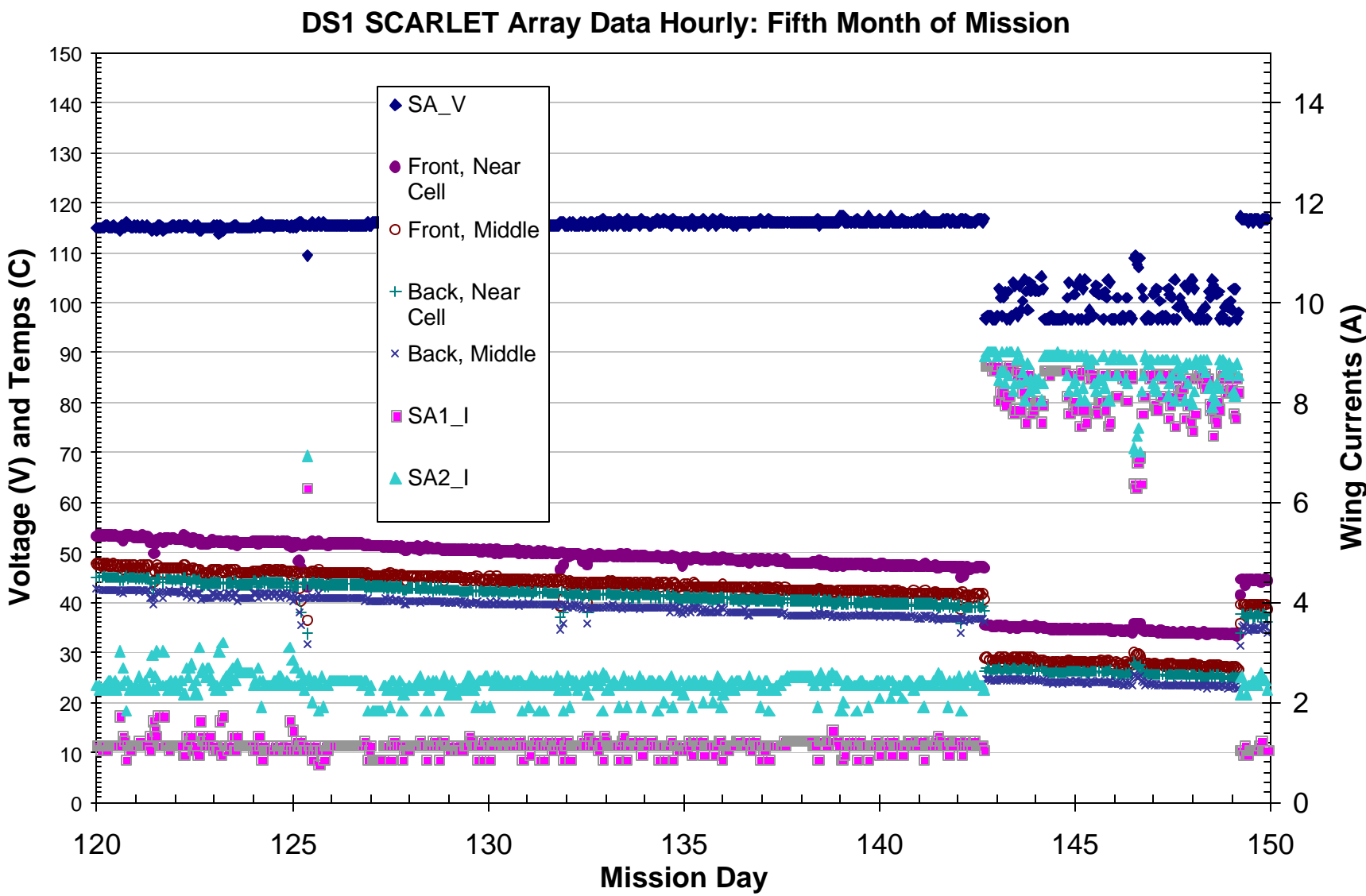


Figure B-6. DS1 SCARLET Array Data Hourly: Fifth Month of Mission

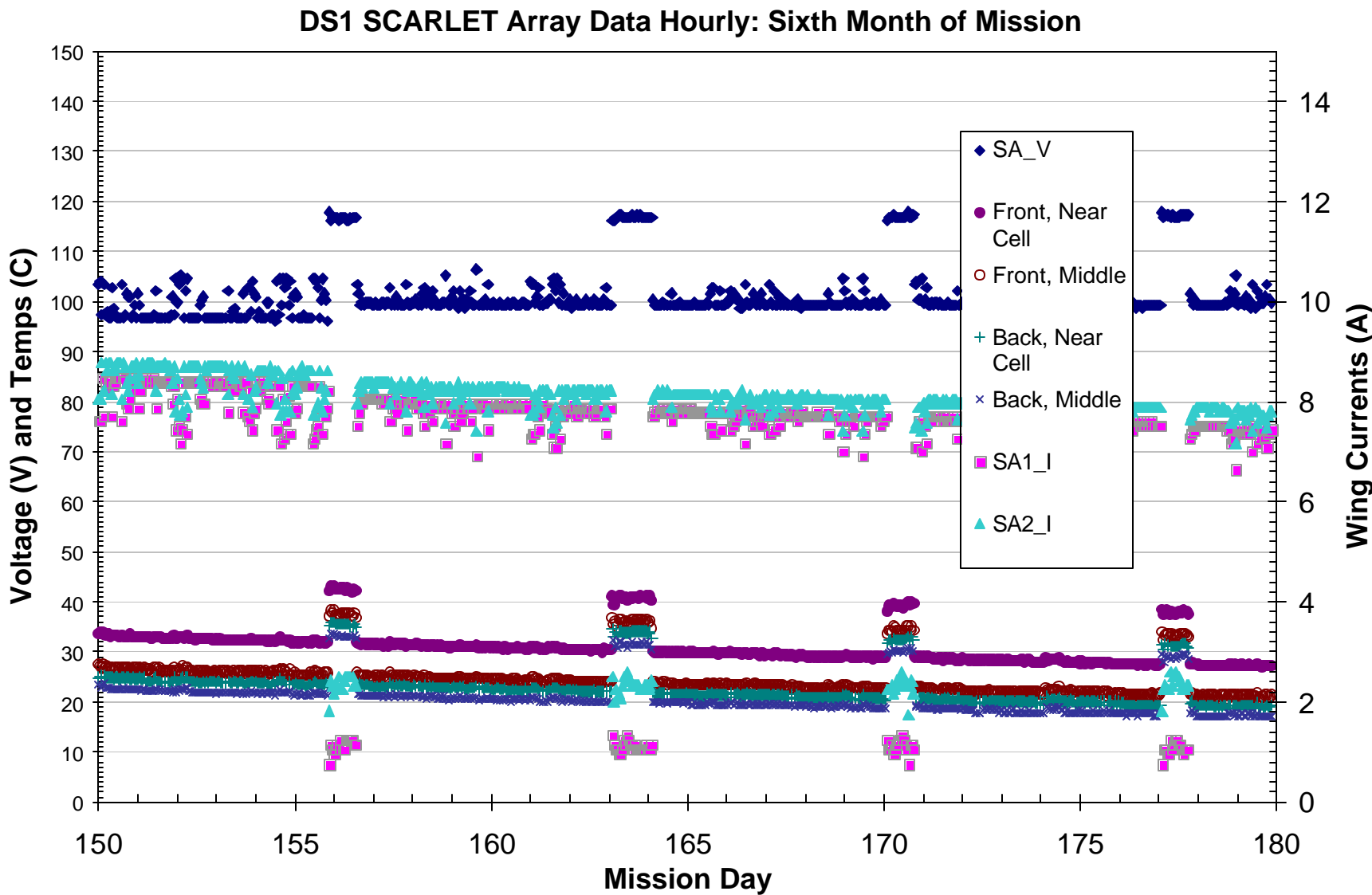


Figure B-7. DS1 SCARLET Array Data Hourly: Sixth Month of Mission

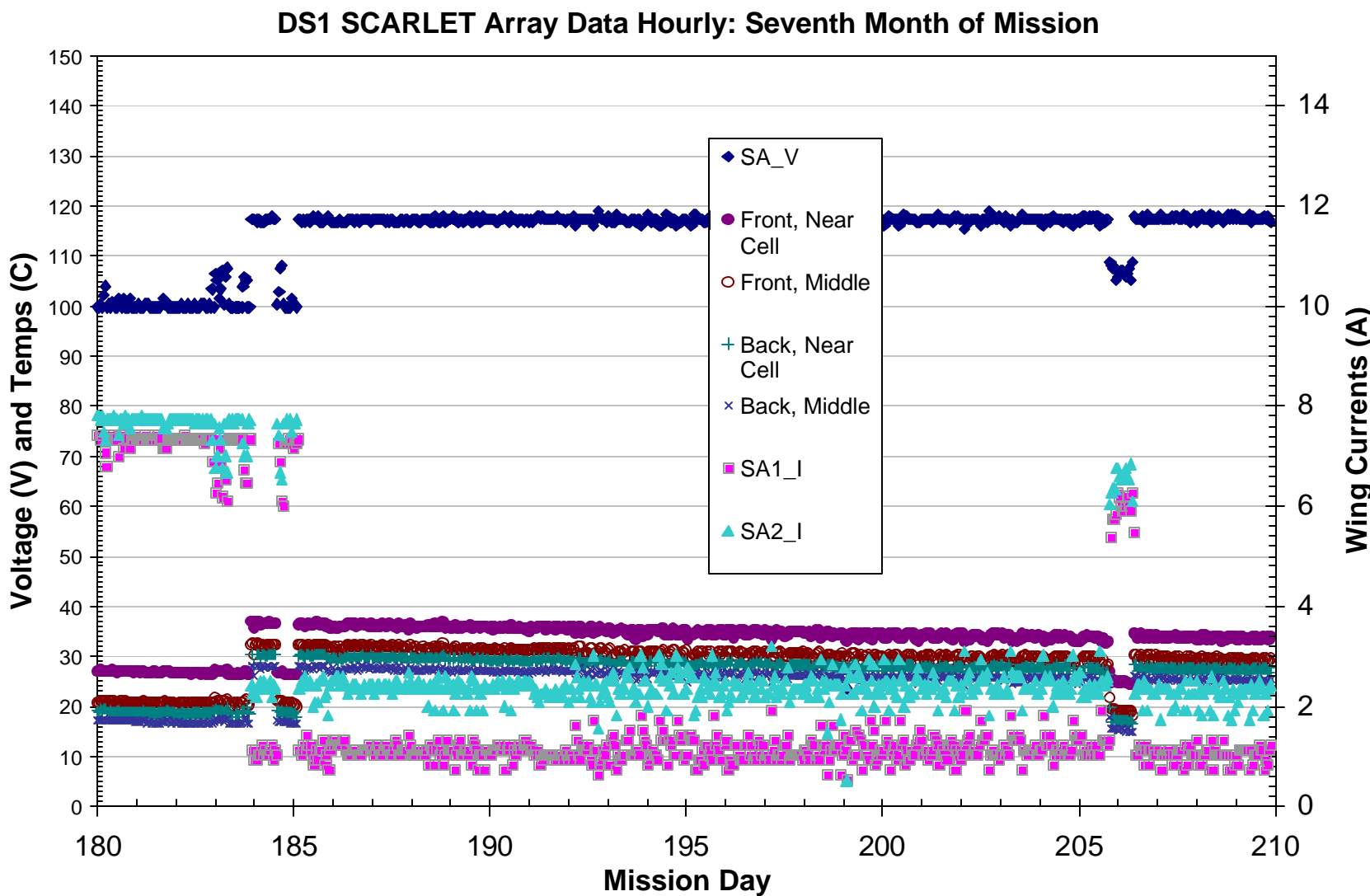


Figure B-8. DS1 SCARLET Array Data Hourly: Seventh Month of Mission

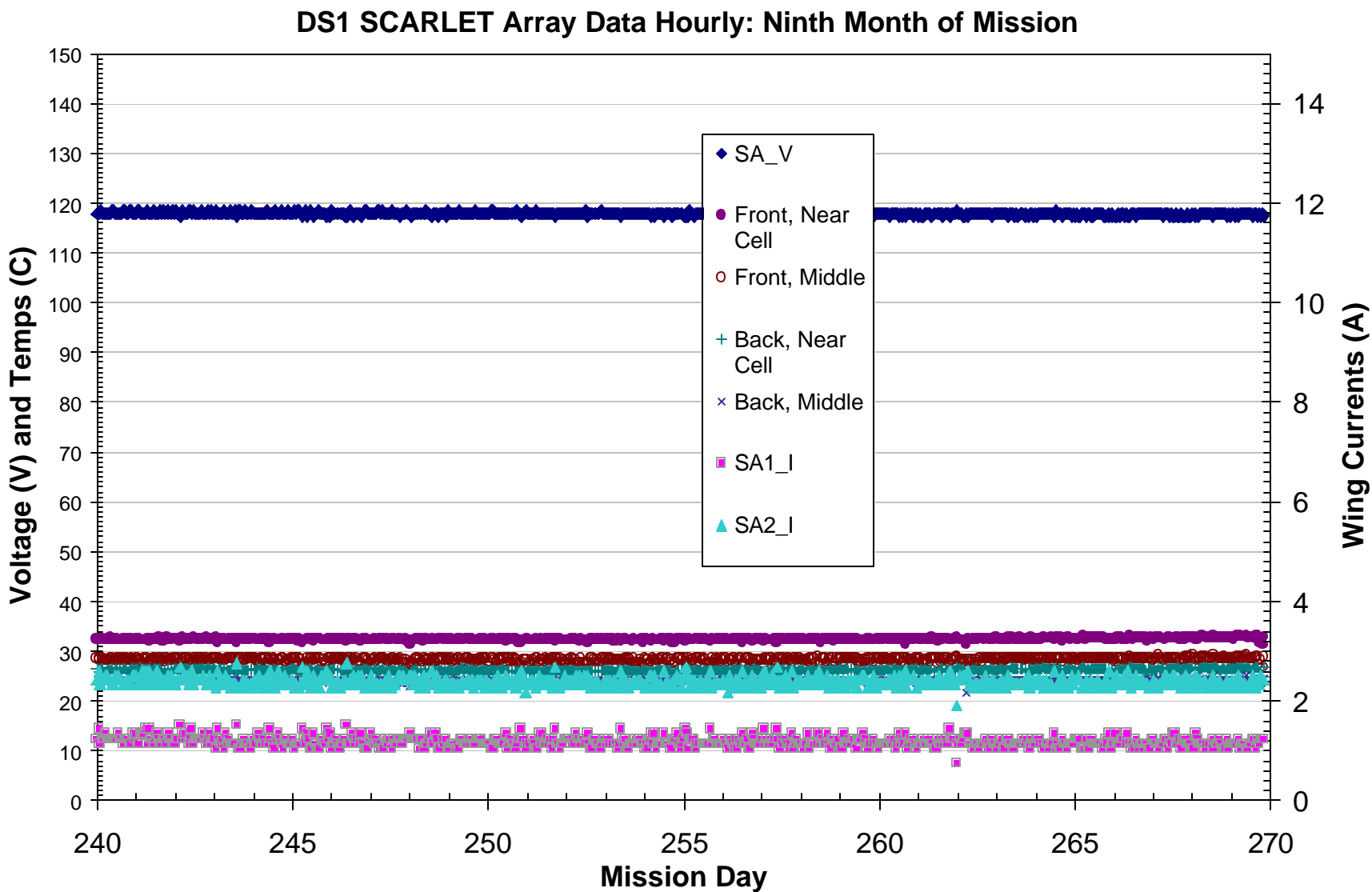


Figure B-9. DS1 SCARLET Array Data Hourly: Ninth Month of Mission

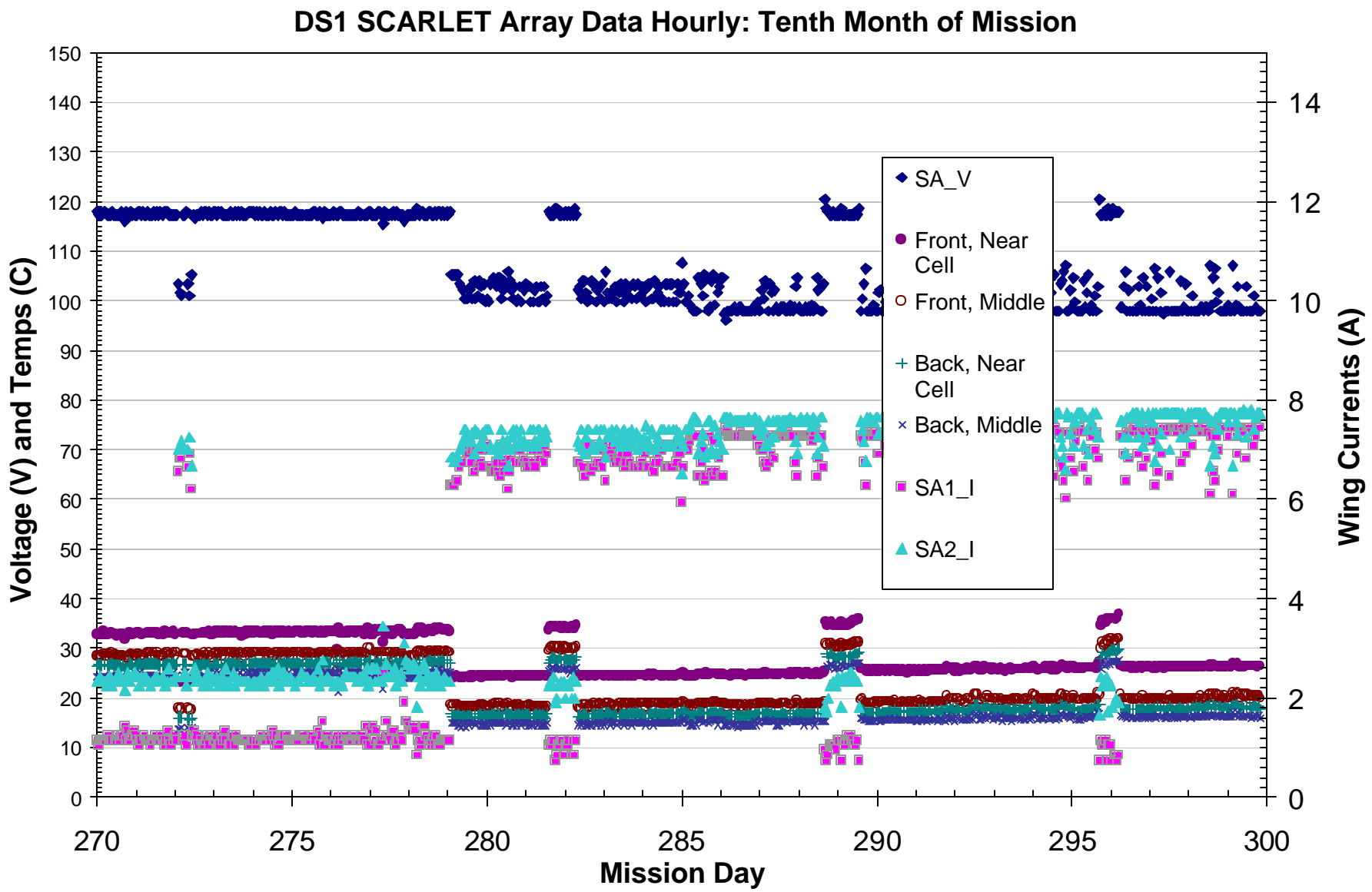


Figure B-10. DS1 SCARLET Array Data Hourly: Tenth Month of Mission

